RESEARCH ARTICLE

Plastidial Phosphoglucose Isomerase is an Important Determinant of Seed Yield through its Involvement in Gibberellin-mediated Reproductive Development and Storage Reserve Biosynthesis in Arabidopsis

Abdellatif Bahaji[1]*, Goizeder Almagro[1]*, Ignacio Ezquer[2]*, Samuel Gámez-Arcas[1], Ángela María Sánchez-López[1], Francisco José Muñoz[1], Ramón José Barrio[3], M. Carmen Sampedro[4], Nuria De Diego[5], Lukáš Spíchal[5], Karel Doležal[5,6], Danuše Tarkowská[6], Elisabetta Caporali[2], Marta Adelina Mendes[2], Edurne Baroja-Fernández[1] and Javier Pozueta-Romero[1]

(1) Instituto de Agrobiotecnología (CSIC/UPNA/Gobierno de Navarra). Iruñako etorbidea 123, 31192 Mutiloabeti, Nafarroa, Spain
(2) Dipartimento di BioScienze, Università degli Studi di Milano, Via Celoria 26, 20133 Milan, Italy
(3) Department of Analytical Chemistry, Faculty of Pharmacy, University of the Basque Country, UPV/EHU, E-01006 Vitoria-Gasteiz, Spain
(4) Central Service of Analysis of Alava, SGIker, University of the Basque Country, UPV/EHU, E-01006 Vitoria-Gasteiz, Spain
(5) Department of Chemical Biology and Genetics, Centre of the Region Haná for Biotechnological and Agricultural Research, Faculty of Science, Palacký University, Olomouc, CZ-78371, Czech Republic
(6) Laboratory of Growth Regulators, Centre of the Region Haná for Biotechnological and Agricultural Research, Institute of Experimental Botany AS CR and Faculty of Science, Palacký University, Šlechtitelů 27, CZ-78371 Olomouc, Czech Republic
* A.B., G.A. and I.E. contributed equally to this work
Corresponding Author: javier.pozueta@unavarra.es

Short title: PGI1 contributes to seed yield

One sentence summary: Plastidial phosphoglucose isomerase determines seed yield by affecting gibberellin-mediated reproductive development and the conversion of glucose-6-phosphate to seed fatty acids and proteins.

The author responsible for distribution of materials integral to the findings presented in this article in accordance with the policy described in the Instructions for Authors (www.plantcell.org) is Javier Pozueta-Romero (javier.pozueta@unavarra.es)

ABSTRACT

The plastid-localized phosphoglucose isomerase isoform PGI1 is an important determinant of growth in *Arabidopsis thaliana*, likely due to its involvement in the biosynthesis of plastidial isoprenoid-derived hormones. Here, we investigated whether PGI1 also influences seed yields. *PGI1* is strongly expressed in maturing seed embryos

and vascular tissues. *PGI1*-null *pgi1-2* plants had ca. 60% lower seed yields than wild type (WT) plants, with reduced numbers of inflorescences and thus fewer siliques and seeds per plant. These traits were associated with low bioactive gibberellin (GA) contents. Accordingly, WT phenotypes were restored by exogenous GA application. *pgi1-2* seeds were lighter and accumulated ca. 50% less fatty acids (FAs) and ca. 35% less protein than WT seeds. Seeds of cytokinin-deficient plants overexpressing *CYTOKININ OXIDASE/DEHYDROGENASE1* (35S:AtCKX1) and GA-deficient *ga20ox1 ga20ox2* mutants did not accumulate low levels of FAs, and exogenous application of the cytokinin BAP and GAs did not rescue the reduced weight and FA content of *pgi1-2* seeds. Seeds from reciprocal crosses between *pgi1-2* and WT plants accumulated WT levels of FAs and proteins. Therefore, PGI1 is an important determinant of Arabidopsis seed yield due to its involvement in two processes: GA-mediated reproductive development and the metabolic conversion of plastidial glucose-6-phosphate to storage reserves in the embryo.

INTRODUCTION

Oilseeds are major sources of calories for human consumption and are of a significant agricultural and industrial value. Seed number and weight are the two main components of seed yield. However, the genetic factors and the molecular and biochemical mechanisms controlling these agronomic traits are still poorly understood (van Daele et al., 2012).

Isoprenoid hormones such as cytokinins (CKs) and gibberellins (GAs) regulate many aspects of plant growth, development and metabolism, including shoot branching and elongation, shoot and reproductive meristem activity, the transition from vegetative growth to flowering, ovule formation, seed development, and the accumulation of seed storage compounds and thus seed yield (Fleet and Sun, 2005; Riefler et al., 2006; Rieu et al., 2008b; Mutasa-Göttgens and Hedden, 2009; Bartrina et al., 2011; D´Aloia et al., 2011, Chen et al., 2012a; Yamaguchi et al., 2014). In plants, these hormones are synthesized from precursors produced in the cytosol by the mevalonate (MVA) pathway and in plastids by the methylerythritol 4-phosphate (MEP) pathway. The MEP pathway uses the central carbon intermediates pyruvate and glyceraldehyde 3-phosphate (GAP) to produce isopentenyl diphosphate and dimethylallyl diphosphate (DMAPP), the universal prenyl diphosphate precursors of all isoprenoids (Pulido et al., 2012; Pokhilko et al., 2015).

In oleaginous species, lipids and proteins are major contributors to seed dry weight and are thus important determinants of yield (Baud et al., 2008). Maturing oilseed

embryos convert sucrose obtained from maternal tissues to lipids and proteins, which are used to support postgerminative seedling growth and establishment. *De novo* synthesis of fatty acids (FA) is an ATP and NAD(P)H-dependent process that is initiated in plastids (Baud et al., 2008). Analyses of expressed sequence tags from developing seeds (White et al., 2000) and microarrays of genes expressed in seeds (Girke et al., 2000; Ruuska et al., 2002) have suggested that the major route of FA biosynthesis in the model oilseed species *Arabidopsis thaliana* involves the glycolytic conversion of sucrose to phosphoenolpyruvate (PEP) and pyruvate in the cytosol. PEP is then transferred to plastids by the plastidial PEP translocator (PPT) and converted to pyruvate via the action of pyruvate kinase (PK). Genetic support for this view has been obtained from characterization of mutants impaired in cytosolic GAP dehydrogenase (GAPDH), PPT and plastid-localized PK (Baud et al., 2007; Prabhakar et al., 2010; Guo et al., 2014). Seeds of these mutants accumulate lower levels of FAs than wild type (WT) seeds. Recently, Lee et al. (2017) reported that seed-specific overexpression of the pyruvate transporter BASS2 increases oil content in Arabidopsis seeds, suggesting that the transport of cytosolic pyruvate into the chloroplast plays an important role in FA biosynthesis. However, metabolic flux analyses have shown that, in oilseed rape (*Brassica napus*) and developing Arabidopsis embryos, large proportions of FAs are synthesized from glucose-6-phosphate (G6P) in plastids via the action of phosphoglucose isomerase (PGI) coupled with pathways involving glycolysis/oxidative pentose phosphate pathway (OPPP*)*/Calvin-Benson enzymes (Schwender et al., 2004; Lonien et al., 2009).

PGI catalyzes the reversible isomerization of fructose-6-phosphate (F6P) and G6P. This enzyme is involved in early steps of glycolysis and is thus important in the generation of ATP, reductants and precursors (amino acids) for protein biosynthesis. PGI is also involved in the regeneration of G6P pools in the oxidative pentose phosphate OPPP, which provides metabolic intermediates for the synthesis of RNA, DNA, phenolic compounds, aromatic amino acids and NADPH. Arabidopsis has two PGI isozymes, one in the cytosol (cytPGI) and the other in the plastid (PGI1) (Yu et al., 2000; Bahaji et al., 2015). It is widely accepted that PGI1 plays a key role in transitory starch biosynthesis in mesophyll cells of leaves, connecting the Calvin-Benson cycle with the starch biosynthetic pathway (Yu et al., 2000). We have shown that Arabidopsis mutants

impaired in PGI1 accumulate low levels of CKs derived from the MEP pathway, display reduced photosynthetic capacity and slow growth phenotypes, and accumulate low levels of transitory starch in leaves, a phenotype that can be reverted to WT by supplementation with exogenous CK (Bahaji et al., 2015). Stimulation of photosynthesis and synthesis of active CK forms is accompanied by enhanced growth and the accumulation of exceptionally high levels of starch in the mesophyll cells of PGI1 null *pgi1-2* plants (Sánchez-López et al., 2016). Thus, we have proposed that PGI1 is an important determinant of photosynthesis, transitory starch accumulation and growth, likely due to its involvement in the synthesis of metabolic intermediates, *e.g.* GAP and pyruvate, required for the synthesis of plastidial isoprenoid-derived molecules (Bahaji et al., 2015).

While PGI1 appears to be involved in the production of precursors and reductants for plastidial isoprenoid-derived hormones and storage reserves such as proteins and FA and could thus potentially be a determinant of yield, its role in these processes has not been clarified through direct genetic tests. The purpose of this study was to investigate the contribution of PGI1 to seed yield via its involvement in GA metabolism, protein and FA biosynthesis. To this end, we investigated the expression pattern of *PGI1* and characterized *pgi1-2* plants. Our results show that PGI1 is an important determinant of seed yield in Arabidopsis due to its involvement in two processes: GA-mediated reproductive development and the metabolic conversion of plastidial G6P to embryonic FA and proteins.

RESULTS

PGI1 is strongly expressed in vascular tissues and developing embryos

We analyzed *PGI1* tissue expression profiles in WT (Ws-2) plants by qRT-PCR and histochemically analyzed WT plants transformed with constructs carrying the *PGI1* promoter region (1700 bp) fused to the β-glucuronidase (GUS) reporter. As shown in **Figure 1A**, qRT-PCR analyses revealed that *PGI1* is weakly expressed in mature leaves and silique envelopes but strongly expressed in roots, stems, flowers and maturing embryos. Zymogram analyses of PGI activity further confirmed that PGI1 is expressed in maturing embryos (**Figure 1B**). Histochemical analyses of 10 independent *promPGI1:GUS*-expressing lines showed that the *PGI1* promoter is strongly active in

vascular tissues of roots, cotyledons and hypocotyls of young seedlings (**Figure 1C$_1$**). It is also active in vascular tissues of fully expanded mature leaves (**Figures 1C$_2$** and **1C$_3$**), roots (**Figures 1C$_2$** and **1C$_4$**) and sepals (**Figure 1C$_5$**). The *PGI1* promoter did not drive expression in anthers, pollen grains or seed coat (**Figure 1C$_5$**) and was weakly active in embryos at the heart developmental stage (**Figure 1C$_6$**), but strongly active in maturing embryos (**Figures 1C$_7$** and **1C$_8$**). In keeping with findings of Tsai et al. (2009, cf. Fig. 5), the *PGI1* promoter was expressed at sub-detection limits in mesophyll cells of mature leaves (**Figures 1C$_2$ and 1C$_3$**). However, this was sufficient for normal starch synthesis in leaf mesophyll cells, as mature leaves of *pgi1-2* plants ectopically expressing *PGI1* under the control of its own promoter (*promPGI1:PGI1* plants) accumulated WT starch levels (**Supplemental Figure 1**).

Knocking out *PGI1* decreases seed yield

To investigate the effects that a lack of PGI1 would have on seed yield, we compared the seed weight per plant at maturity between Ws-2 and *pgi1-2* plants. We also characterized *aps1* plants impaired in the small subunit of ADP-glucose pyrophosphorylase (Ventriglia et al, 2008), which, like *pgi1-2* plants, show a slow growth phenotype when cultured under long day conditions and accumulate low levels of transitory starch in their leaves (Bahaji et al., 2015). As shown in **Table 1**, we found that seed yields of *pgi1-2* plants were only ca. 40% of those of WT plants, but WT yields could be restored by ectopic expression of *PGI1* under its own promoter or the 35S promoter (**Table 1**). In clear contrast, *aps1* plants had similar to WT seed yields (**Table 1**).

Knocking out *PGI1* reduces the number of seeds per plant

The reductions in seed yields of *pgi1-2* plants could potentially be due to reductions in seed weight or in the number of either seeds per silique or siliques per plant. To differentiate between these possibilities we first counted the numbers of inflorescences and siliques per plant and the numbers of seeds per silique in WT (Ws-2) and *pgi1-2* plants. We also characterized *aps1* plants. At first sight, we detected no major differences between the external phenotypes of Ws-2 and *pgi1-2* plants at maturity (**Figure 2A**). Additionally, there was no significant difference in the number of seeds per silique

between Ws-2 and *pgi1-2* plants (**Table 1**). However, many inflorescences failed to elongate in *pgi1-2* plants, and flowers developing first on the raceme exhibited short anthers and failed to produce siliques and seeds (**Figure 2B**). Consequently, the numbers of inflorescences with siliques and siliques per plant were lower in *pgi1-2* plants than in Ws-2 plants (**Table 1**), thus causing a reduction in the number of seeds per plant. This phenotype could be rescued by the ectopic expression of *PGI1* under the control of its own promoter or the 35S promoter (**Table 1**). Contrary to *pgi1-2*, *aps1* plants had similar numbers of inflorescences and siliques per plant to WT plants (**Table 1**). These results demonstrate that PGI1 is an important determinant of seed yield, at least partly because of its involvement in reproductive development.

The reduced number of inflorescences in the *pgi1-2* mutant is associated with low bioactive GA content

We have reported that *pgi1-2* plants accumulate lower than WT-levels of MEP-derived CKs and proposed that PGI1 may be involved in the production of precursors of MEP-pathway-derived isoprenoid compounds (Bahaji et al., 2015). As GAs and CKs are important determinants of reproductive development (Rieu et al., 2008a,b; Bartrina et al., 2011), we hypothesized that the reduction in the numbers of elongated inflorescences, well-developed flowers, siliques and seeds in *pgi1-2* plants could be at least partly due to reduced contents of these isoprenoid hormones. To explore this possibility further, we measured levels of different GAs in shoots (all aerial parts including rosette) at bolting time in Ws-2, *pgi1-2* and *promPGI1:PGI1* plants. We also counted the numbers of inflorescences and siliques in Ws-2 and *pgi1-2* plants following exogenous 6-benzylaminopurine (BAP) or GA_{4+7} application.

Notably, levels of GA_1, GA_3 and GA_4 –the main bioactive GAs in plants (Yamaguchi, 2008; Hedden and Thomas, 2012)– were lower in *pgi1-2* shoots than in Ws-2 shoots, but WT levels could be restored by ectopic expression of *PGI1* (**Figure 3**). Also, *pgi1-2* plants accumulated higher levels of the inactive catabolites GA_{29} and GA_8 than Ws-2 plants and *promPGI1:PGI1*-expressing *pgi1-2* plants (**Figure 3**). Moreover, exogenous application of GA_{4+7} restored to WT the numbers of elongated inflorescences and siliques of the *pgi1-2* mutant (**Table 2**). In contrast, exogenously applied BAP did

not affect the number of inflorescences and siliques (**Table 2)**. The overall data provide strong evidence that PGI1 is an important determinant of bioactive GA content, and they indicate that the low number of inflorescences, siliques and seeds in *pgi1-2* plants is at least partly due to lower levels of active GA forms.

GA_1 and GA_4 are produced by the GA3-oxidase (GA3ox)-mediated oxidation of GA_{20} and GA_9, respectively (**Figure 3**). These bioactive GAs can be deactivated by GA2-oxidase (GA2ox), yielding GA_8 and GA_{34}, respectively (Yamaguchi, 2008; Hedden and Thomas, 2012) (**Figure 3**). GA2ox can also metabolize GA_{20} to the inactive GA_{29} (Hedden and Thomas, 2012). In Arabidopsis shoots, the most strongly expressed GA2ox- and GA3ox-encoding genes are *GA2ox6* and *GA3ox1,* respectively (Mitchum et al., 2006; Rieu et al., 2008a). Whereas *GA3ox1* is up-regulated by CKs, *GA2ox6* is down-regulated by these hormones (Kiba et al., 2005; Bhargava et al., 2013; Brenner and Schmülling, 2015). This and the findings that *pgi1-2* plants accumulate low levels of CKs (Bahaji et al., 2015) would suggest that the reduced contents of bioactive GAs and enhanced levels of inactive GAs in *pgi1-2* plants could be due to reductions in *GA3ox1* and/or increases in *GA2ox6* expression caused by the reduced CK content. To investigate this hypothesis, we conducted qRT-PCR analyses of *GA2ox* and *GA3ox* genes in shoots at bolting time in Ws-2 and *pgi1-2* plants. We also analyzed the expression levels of *GA20ox* genes. As shown in **Supplemental Figure 2**, no significant differences in the expression levels of these genes were found between WT and *pgi1-2* shoots.

Knocking out *PGI1* decreases seed weight and the contents of proteins and fatty acids

We next addressed the possibility that the low seed yields of *pgi1-2* plants could also be related to reductions in seed weight. As shown in **Table 1**, *pgi1-2* seeds were 35% lighter than Ws-2 seeds, but WT weights could be restored by ectopic expression of *PGI1*. Analyses of embryonic phenotypes in a series of developing pollinated pistils revealed no major differences between *pgi1-2* seeds and Ws-2 seeds (**Supplemental Figure 3**) excluding the possibility that the reduced weight of *pgi1-2* seeds could be due to aberrant embryo growth and development. Dry *pgi1-2* seeds displayed a wrinkled phenotype (**Figures 4A,B**), accumulated 35% less dry matter than Ws-2 seeds (**Figure 4C**), and had

lower establishment rates on MS agar with no supplemental sugar than WT seeds (**Figure 5**). These phenotypes could be restored by ectopic expression of *PGI1* (**Figures 4** and **5**).

Focks and Benning (1998) suggested that the wrinkled appearance of oil-deficient *wri1-1* seeds could be due to an increased sucrose content during seed development. To determine whether this might be the case in *pgi1-2* seeds, we performed time-course analyses of sucrose levels in developing Ws-2 and *pgi1-2* seeds. As shown in **Supplemental Figure 4**, there were no detectable differences between Ws-2 and *pgi1-2* seeds with respect to their sucrose contents during development.

Oil and proteins are major components of dry Arabidopsis seeds (Baud et al., 2008), and seeds with reduced FA content show a wrinkled phenotype (Focks and Benning, 1998; Baud et al., 2007; Chen et al., 2015). Furthermore, seedlings of mutants with defects in the synthesis or post-germinative mobilization of seed storage lipids have reduced establishment rates in the absence of an exogenous sugar source (Hayashi et al., 1998; Cernac et al., 2006; Baud et al., 2007). Thus, these observations suggested that *pgi1-2* seeds have reduced protein and lipid contents. This inference was corroborated by analysis of protein and FA levels (following methylesterification) in mature seeds. As shown in **Figure 4D** and **E**, *pgi1-2* seeds accumulated ca. 35% less protein and ca. 50% less FA than Ws-2 seeds at maturity, but WT levels could be restored by ectopic expression of *PGI1*. On a dry weight (DW) basis, *pgi1-2* seeds accumulated ca. 8% less protein and 23% less FA than Ws-2 seeds (**Figures 4F** and **G**).

We also analyzed the FA composition in mature *pgi1-2* seeds and, as shown in **Figure 4H**, found no significant differences in relative contents of the saturated FAs palmitic acid (16:0) and stearic acid (18:0) between Ws-2 and *pgi1-2* seeds. In contrast, relative amounts of the desaturation intermediates, oleic (18:1), and linoleic (18:2) acids, were lower in *pgi1-2* seeds than in Ws-2 seeds, while the relative amounts of the end products of desaturation and elongation, linolenic (18:3) and erucic (22:1) acids, were higher (**Figure 4H**). The FA composition profile of *pgi1-2* seeds was similar to that of seeds of the low seed oil *wri1* mutant and plants lacking the plastid-localized PK (Focks and Benning, 1998; Baud et al., 2007). These mutations impair FA biosynthesis by reducing precursor supplies. These findings indicate that PGI1 is an important

207 determinant of seed oil accumulation through its involvement in the provision of
208 precursors for FA synthesis.
209
210 **The low fatty acid content of *pgi1-2* seeds is not due to reduced active GA or CK**
211 **contents**
212 *pgi1-2* plants accumulate low levels of active forms of CKs (Bahaji et al., 2015) and GAs
213 (this work). To determine whether the reduced weight and FA content of *pgi1-2* seeds
214 could be due to low levels of active CKs or GAs, we characterized seeds of CK-deficient
215 plants overexpressing *CYTOKININ OXIDASE/DEHYDROGENASE1* (35S:AtCKX1
216 plants) (Werner et al., 2003) and the GA-deficient *ga20ox1 ga20ox2* double mutant (Rieu
217 et al., 2008b). Furthermore, we characterized seeds of *pgi1-2* plants treated with
218 exogenous BAP or GA_{4+7}. In keeping with the findings of Werner et al. (2003),
219 35S:AtCKX1 seeds were enlarged (**Figure 6A**) and had almost twice the mass of WT
220 seeds (**Figure 6B**) due to the role of CKs in controlling the cell division rate in maturing
221 embryos (Werner et al., 2003). Additionally, the FA content of 35S:AtCKX1 seeds was
222 twice that of WT seeds (**Figure 6C**). Conversely, the size, weight and FA content of
223 *ga20ox1 ga20ox2* seeds were comparable to those of WT seeds (**Figure 6A,B,C**).
224 Moreover, treatment with exogenous BAP and GA_{4+7} did not rescue the reduced weight
225 and FA content phenotypes of *pgi1-2* seeds (**Figure 6D,E**), showing that the low FA
226 content of *pgi1-2* seeds is not due to reduced active GA or CK contents.
227
228 **PGI1 zygotically controls FA and protein accumulation**
229 Protein and FA contents in Arabidopsis seeds can be influenced by diverse maternal
230 factors. For examples, reductions in maternal carbon supplies may cause reductions in FA
231 accumulation in seeds (Chen et al., 2015). Proteins involved in regulating flavonoid
232 biosynthesis in the seed coat can affect seed oil deposition by down-regulating embryonic
233 FA biosynthetic genes (Chen et al., 2012b; 2014). In addition, the homeotic regulatory
234 gene *APETALA2* can affect seed oil and protein accumulation through its action in the
235 maternal sporophyte and endosperm genomes (Jofuku et al., 2005). *pgi1-2* plants have
236 reduced photosynthesis rates (Bahaji et al., 2015), so their low seed protein and FA
237 contents could potentially be due to maternal factors such as limited photosynthate

supplies or signals from maternal tissues. To test this possibility, we performed reciprocal crosses between *pgi1-2* and Ws-2 plants and analyzed the percentages of wrinkled seeds, protein and fatty acid methylester (FAME) contents in seeds of the F1 progeny. As shown in **Figure 7**, there was no significant difference in the percentage of wrinkled seeds and seed FA and protein contents between the progeny of Ws-2 plants and *pgi1-2* and Ws-2 crosses, showing that the low FA and protein contents of *pgi1-2* seeds is dependent on the embryonic genotype but not on factors from the maternal tissues.

Plastidial phosphofructokinase-mediated metabolism of F6P produced by PGI1 is not absolutely required for normal fatty acid biosynthesis in Arabidopsis

Schwender et al. (2004) comprehensively delineated every possible conversion of G6P entering the plastid into FAs in oil seed embryos using a network model consisting of glycolysis, the OPPP, the Calvin-Benson cycle, and FA synthesis enzymes. The study revealed seven flux modes that include RubisCO and that have higher carbon use efficiencies than glycolysis, two of which (modes 16 and 18) involve ATP-dependent phosphofructokinase (PFK) and bypass the glycolytic steps catalyzed by GAPDH and phosphoglycerate kinase (PGK). Two other modes (24 and 25) also have zero flux through PFK (Schwender et al., 2004). To determine whether plastidial PFK-mediated metabolism of F6P produced by PGI1 is absolutely required for normal seed FA synthesis, we measured the FA contents in seeds of the *pfk4 pfk5* double knock-out mutant of Arabidopsis, which has impairments in the two plastidial PFK isoforms expressed in Arabidopsis (one active, PFK4, and the other, PFK5, having weak activity when transiently expressed in wild tobacco (*Nicotiana benthamiana*) plants; **Supplemental Figure 5**). We reasoned that if the plastid-localized PFK is absolutely required for the G6P-to-FA conversion, *pfk4 pfk5* seeds should accumulate low levels of FAs. Conversely, if the plastid-localized PFK-mediated metabolism of F6P produced by PGI1 is not absolutely required for normal FA biosynthesis, *pfk4 pfk5* seeds should not accumulate low levels of FAs. As shown in **Figure 8**, the latter prediction was verified: *pfk4 pfk5* seeds displayed a WT external phenotype and did not accumulate low levels of FA.

DISCUSSION

PGI1 is expressed in organs that produce active GAs and MEP-pathway derived CKs

We have proposed that PGI1 could be involved in the glycolytic conversion of plastidial G6P into GAP and pyruvate necessary for the synthesis of plastidial isoprenoid-derived hormones, as schematically illustrated in **Figure 9A** (Bahaji et al., 2015). The results presented here consistently indicate that *PGI1* is expressed in organs expressing genes associated with the biosynthesis of GA and MEP pathway-derived CKs. In particular, this gene is expressed in vascular tissues (**Figure 1**), like genes such as *GA1* (which encodes the enzyme that catalyzes the first committed step of GA biosynthesis, the *ent*-copalyl diphosphate synthase [CPS]), *GA3ox1* and *GA3ox2* (which encode enzymes that catalyze the production of bioactive GAs), and several genes encoding enzymes involved in rate-limiting steps of plastidial CK biosynthesis (Silverstone et al., 1997; Miyawaki et al., 2004; Mitchum et al., 2006). The strikingly similar expression patterns of *PGI1* and these genes involved in the synthesis of active GAs and CKs would suggest that primary carbohydrate metabolism and secondary isoprenoid metabolism in plastids are transcriptionally co-regulated via mechanisms that harmonize GA and CK biosynthesis rates (and thus growth and development-related processes) with carbon supplies. Accordingly, like *PGI1* and some genes involved in the synthesis of plastidial isoprenoid-derived hormones, *PPT1* and *PKp2* (both encoding enzymes that function in the provision of pyruvate to the plastid) are expressed in vascular tissues of adult plants and seedlings (Knappe et al., 2003; Baud et al., 2007).

Environmental stimuli such as light, temperature and salt stress specifically regulate the expression of GA biosynthetic enzymes, allowing GAs to translate these extrinsic signals into developmental changes according to environmental conditions (Yamaguchi, 2008). Oxidative modification of redox-sensitive proteins plays important roles in modulating rapid physiological and developmental responses of plants to changing environmental conditions (Foyer and Noctor, 2005). Notably, recent high-throughput analyses of proteins whose thiols undergo reversible oxidative modifications in Arabidopsis have revealed that PGI1 is a redox-sensitive protein that responds to agents that perturb cellular redox homeostasis and inhibit growth (Liu et al., 2014; Yin et

al., 2017). It is thus tempting to speculate that PGI1 could play an important role in fine regulatory tuning of plastidial isoprenoid hormone-driven growth to a pace that is compatible with the plant's carbon status under prevailing environmental conditions.

PGI1 is an important determinant of seed yield due to its involvement in GA-mediated reproductive development

pgi1-2 plants produce fewer elongated inflorescences than Ws-2 plants, and flowers developing first on the short inflorescences fail to produce siliques and seeds (**Figure 2B**). Consequently, *pgi1-2* plants produce fewer siliques and seeds than Ws-2 plants (**Table 1**). This phenotype cannot be ascribed to slow plant growth or low leaf starch content, since the number of inflorescences and the seed yield of starch-deficient *aps1* plants were comparable to those of WT plants (**Table 1**).

In Arabidopsis, bioactive GAs stimulate elongation of vegetative stem internodes upon bolting and exert a positive effect on inflorescence length and flower formation, thus acting as major determinants of reproductive development and yield (Rieu et al., 2008b; Yamaguchi et al., 2014). Here we have shown that levels of the main bioactive GAs (*e.g.* GA_1, GA_3 and GA_4) are lower in *pgi1-2* plants than in Ws-2 plants and *pgi1-2* plants ectopically expressing *PGI1* (**Figure 3**). These findings strongly indicate that the reduced numbers of elongated inflorescences, siliques and seeds per *pgi1-2* plant are partly due to their diminished content of active GAs. Accordingly, exogenous GA application restored to WT the numbers of elongated inflorescences and siliques in *pgi1-2* plants (**Table 2**). Therefore, we propose that PGI1 is a major determinant of seed yield, at least in part, due to its regulatory action on GA homeostasis and thus reproductive development.

To maintain optimum growth rates, plants have evolved homeostatic regulatory mechanisms for modulating GA levels involving both negative feedback and positive feed-forward transcriptional regulation of GA metabolism genes (Hedden and Thomas, 2012). Plants have also evolved less well-defined mechanisms for post-transcriptional regulation of GA metabolism that may involve microRNA-mediated destabilization and/or reductions in the efficiency of translation of several *GA2ox, GA3ox* and *GA20ox* transcripts (http://sundarlab.ucdavis.edu/mirna/) (Barker, 2011) and modification of the

stability of GA metabolism enzymes (Magome et al., 2004; Lee and Zeevaart, 2007; Barker, 2011). The qRT-PCR analyses conducted in this study revealed no major differences in the expression of GA metabolism genes between Ws-2 and *pgi1-2* plants that could account for the observed differences in the GA contents of these genotypes (**Supplemental Figure 2**). This finding suggests that there are further complexities in GA homeostasis due to mechanisms in which PGI1 plays an important role in regulating the activity of GA metabolism enzymes and/or providing precursors for active GA biosynthesis.

PGI1 is an important determinant of seed yield due to its involvement in embryonic fatty acid and protein biosynthesis

PGI1's roles in seed FA and protein production have previously been obscure. Here we have provided evidence that PGI1 contributes to seed yield through participation in the generation of precursors for embryonic FA and protein biosynthesis, as schematically illustrated in **Figure 9B**. The hypothesis is strongly supported by the following findings: *pgi1-2* seeds accumulate ca. 35% less protein and 50% less FAs than Ws-2 seeds, respectively (**Figure 4**), *PGI1* is strongly expressed in the embryo (**Figure 1**), and *PGI1* zygotically controls FA and protein accumulation (**Figure 7**). Two findings strongly indicate that the low FA contents of *pgi1-2* seeds are not due to reduced active CK and GA contents: seeds of CK-deficient 35S:AtCKX1 and GA-deficient *ga20ox1 ga20ox2* do not accumulate low levels of FA (**Figure 6C**), and exogenous application of BAP and GA_{4+7} did not rescue the reduced weight and FA content of *pgi1-2* seeds (**Figure 6D,E**). The observation that *pgi1-2* seeds have elevated relative contents of linolenic and erucic acids (**Figure 4H**) indicates that no feedback regulation occurs in this mutant to adjust the degree of unsaturation and elongation of the FAs to the decrease of carbon flow into the FA biosynthetic pathway, and that different regulators control the activities of enzymes involved in lipid metabolism during seed development.

PGI may be involved in regenerating the G6P pool in the OPPP or early steps of glycolysis. The plastidial OPPP has been regarded as one of the major sources of NADPH linked to FA biosynthesis in oilseeds (Kang and Rawsthorne, 1996; Eastmond and Rawsthorne, 1998; Hutchings et al., 2005). An objection to this hypothesis is that

362 plastid-localized G6P dehydrogenase (which catalyzes G6P's entry into the plastidial
363 OPPP) is subject to redox inactivation during illumination (Née et al., 2009), so plastidial
364 G6P dehydrogenase is likely inactive during FA accumulation in green oilseeds.
365 Furthermore, metabolic flux analyses have indicated that the reductant produced by the
366 plastidial OPPP accounts for only 20% of the total reductant needed for FA synthesis in
367 oilseed embryos (Schwender et al., 2003). The glycolytic capacity in plastids of lipid-
368 storing seeds considerably exceeds requirements for maximum rates of lipid synthesis
369 (Eastmond and Rawsthorne, 2000). Thus, the glycolytic pathway could play an important
370 role in the conversion of photosynthate to oil. However, previous biochemical analyses
371 with oilseed rape and Arabidopsis embryos have shown that up to 80% of the 3PGA
372 linked to FA biosynthesis is generated from G6P through pathways involving
373 glycolysis/OPPP/Calvin-Benson enzymes that have higher carbon use efficiencies than
374 glycolysis (Schwender et al., 2004; Lonien et al., 2009). Some of these pathways involve
375 plastidial PFK. Others have zero flux through PFK and derive the GAP needed for Ru5P
376 production via 3PGA metabolism (Schwender et al., 2004; Lonien et al., 2009). In this
377 work, we found that *pfk4 pfk5* seeds do not accumulate low levels of FA (**Figure 8C**),
378 strongly indicating that plastidial PFK is not absolutely required for the metabolic
379 conversion of F6P produced by PGI1 into FAs in Arabidopsis seeds. To explain why the
380 *pgi1-2* mutation reduces seed FA content but the *pfk4 pfk5* mutation does not, we propose
381 that *pgi1-2* completely blocks the entry of carbon into the 3PGA-generating
382 glycolysis/OPPP/RubisCO network, whereas *pfk4 pfk5* can be compensated for by
383 RubisCO shunt flux modes that cause some 3PGA formed in the plastids to be converted
384 into the GAP needed for Ru5P production by plastidial GAPDH and PGK enzymes
385 (**Figure 9B**). The remainder of the 3PGA produced in the plastids may be metabolized in
386 plastids and/or exported to the cytosol, where it may be converted to PEP and pyruvate,
387 which may move back into plastids and subsequently be converted to FAs (**Figure 9B**).
388 According to a flux map of central carbon metabolism established in steady-state
389 ^{13}C labeling experiments by Schwender et al. (2003), PEP is preferentially transported
390 from the cytosol to the stroma as a substrate for *de novo* FA synthesis in developing
391 rapeseed embryos. The Arabidopsis genome contains two PPT-encoding genes: *PPT1*
392 and *PPT2* (Knappe et al., 2003). Unlike *PPT1, PPT2* is not expressed in seeds (Knappe et

al., 2003) (see also http://bar.utotonto.ca/efp/cgi-bin/efpWeb.cgi; Winter et al., 2007). Although the overall information indicates that PPT1 participates in embryonic FA biosynthesis, Prabhakar et al. (2010) showed that seeds of Arabidopsis *cue1* plants with defective PPT1 can accumulate up to 85% of WT FA contents. This indicates that PEP may not be the major form of photosynthate that enters the plastid for subsequent conversion to FAs in Arabidopsis seeds. Moreover, the findings that *pgi1-2* seeds and seeds of *pkp2* plants impaired in plastidial PK accumulate 50% and 60% less FA than WT seeds, respectively (Baud et al., 2007; this work) strongly indicate that a sizable pool of the photosynthate linked to Arabidopsis seed FA production enters the plastid as G6P and pyruvate, as shown schematically in **Figure 9B**.

METHODS

Plants, growth conditions and sampling

The work was carried out using *Arabidopsis thaliana* WT plants (ecotypes Col-0 and Ws-2), *pgi1-2* knock-out mutants (Bahaji et al., 2015), Ws-2 plants expressing *GUS* under the control of the 1700 bp Ws-2 *PGI1* promoter (*promPGI1:GUS*), *pgi1-2* plants expressing *PGI1* under the control of the 1700 bp *PGI1* promoter (*promPGI1:PGI1*), *pgi1-2* plants expressing *PGI1* under the control of the cauliflower mosaic virus 35S promoter (*35S:PGI1*), the ADPglucose pyrophosphorylase null *aps1* mutant (SALK_040155), *CK OXIDASE/DEHYDROGENASE1* over-expressing 35S:CKX1 plants (Werner et al. 2003), the GA-deficient *ga20ox1 ga20ox2* double mutant (Rieu et al., 2008b) and the *pfk4* and *pfk5* T-DNA insertional knock-out mutants (SALK_012602 and SAIL_297_F05, respectively) obtained from the European *Arabidopsis* Stock Center (NASC). By crossing *pfk4* with *pfk5,* self-pollinating the resulting heterozygous mutants, and PCR-screening for homozygous progeny using the oligonucleotide primers listed in **Supplemental Table 1,** we produced *pfk4 pfk5* double mutants. The *promPGI1:PGI1, 35S:PGI1* and *promPGI1:GUS* plasmid constructs were produced using Gateway technology as illustrated in **Supplemental Figure 6** and confirmed by sequencing. Primers used for PCR amplification of *PGI1* cDNA, *GUS* and the *PGI1* promoter are listed in **Supplemental Table 2**. The plasmid constructs were transferred into *Agrobacterium tumefaciens* EHA105 cells by electroporation and utilized to transform *Arabidopsis*

plants as described by Clough and Bent (1998). Transgenic *promPGI1:PGI1*, *35S:PGI1* and *promPGI1:GUS* plants were selected on medium containing antibiotics.

Plants were cultured on soil in growth chambers under a long-day photoperiod with (16 h light 22°C/8 h dark 18ºC) at 90 μmol photons m^{-2} sec^{-1} light intensity using a mix of Sylvania 215-W cool white fluorescent tubes and 60-W mate bulbs. For exogenous application of CKs and GAs, one week after bolting, *pgi1-2* plants were sprayed every two days with the indicated concentrations of BAP or GA_{4+7}.

Confirmation of the knock-out status of *pfk5*

PFK5 contains 13 exons (**Supplemental Figure 5A**) and encodes a protein of 537 amino acids (**Supplemental Figure 5B**) with weak activity. The *pfk5* allele has a T-DNA inserted in exon 12 and encodes a truncated protein (designated PFK5*) that lacks 85 amino acids at the C-terminus (**Supplemental Figure 5B**). To explore whether PFK5* is enzymatically active, we produced *PFK5*, *PFK5** and *PFK4* expression vectors (**Supplemental Figure 7**). Primers used for PCR amplification of *PFK4* and *PFK5* cDNA are listed in **Supplemental Table 2**. The plasmids were transferred to *A. tumefaciens* GV3101, which were used for transient expression in agro-infiltrated *N. benthamiana* leaves. For co-infiltration of the RNA-silencing inhibitor P19, a bacterial suspension harboring pBin61-P19 (Voinnet et al., 2003) was added. The bacteria were infiltrated into the abaxial sides of leaves using a 1-ml syringe with no needle. *N. benthamiana* leaf samples were taken two days after infiltration, immediately frozen in liquid nitrogen and subjected to ATP-PFK activity measurement analyses as described by Mustroph et al. (2007).

qRT-PCR analyses

Total RNA was extracted from frozen organs using the TRIzol method according to Meng and Feldman (2010) and treated with RNase-free DNase (Takara), then 1.5 μg portions were reverse-transcribed using a mixture of oligo(dT) and random primers and an Expand Reverse Transcriptase kit (Roche) according to the manufacturer's instructions. RT-PCR amplifications were performed using a 7900HT sequence detector system (Applied Biosystems) with Premix Ex Tag Mix (Takara RR420A) according to

the manufacture's protocol. Each amplification was performed in triplicate with 0.4 µL of the first-strand cDNA in a total volume of 20 µL. The specificity of the PCR amplicons was checked by acquiring heat dissociation curves (from 60ºC to 95ºC). Comparative threshold values were normalized to an *EF-1α* RNA internal control and compared to obtain relative expression levels. Primers used for qRT-PCR amplification of *PGI1* and different *GA2ox, GA3ox* and *GA20ox* genes are listed in **Supplemental Table 3**.

GUS expression analysis

Expression of the GUS reporter gene was monitored using the histochemical staining assay described by Jefferson et al. (1987).

Morphological analysis of seeds

Seeds were observed and photographed using an Olympus MVX10 stereomicroscope (Japan). Scanning electron microscopy analyses of gold-coated dry seeds were performed using a JEOL JSM-5610LV scanning electron microscope.

Metabolite analysis

Seed fatty acid content analysis

Sets of 20 dry seeds were prepared in Teflon-lined screw-capped glass tubes and incubated at 90°C for 90 min in 1 mL of 1 M HCl in methanol, with 20 µg of heptadecanoic acid (C17:0) as an internal standard, and 300 µl of toluene. After cooling to room temperature, FAMEs were extracted in 1 mL hexane following the addition of 1.5 mL of 0.9% (w/v) NaCl. The hexane phase was transferred to a gas chromatography vial after vigorous vortex-mixing and centrifuged for 3 min at 10,000 *g*. Portions (1 µl) of the samples were analyzed using a GC-MS system consisting of a 7890A GC equipped with an Agilent J&W DB-WAX column (diameter 0.25 mm, film thickness 0.25 µm, length 30 m) coupled to a 5975C Inert XL MSD mass selective detector (Agilent Technologies, Santa Clara, USA). The GC settings were as follows: carrier gas, helium (1 mL/min); injection mode, split (1:50); injector temperature, 250°C; GC temperature program, 1 min at 50°C then 25°C/min rise to 200°C followed by 3°C/min rise to 230°C and finally 18 min hold at 230°C. The MSD settings were: solvent delay, 5 min; ion

source temperature, 230°C; fragmentation energy, 70 eV; scanning rate, 20 scans/min (40 to 500 m/z). Data were acquired with ChemStation software (Agilent).

Seed protein content analysis

Sets of 200 dry seeds were ground in a mortar and pestle. The powder was resuspended in 60 µl of extraction buffer (50 mM HEPES, 5 mM $MgCL_2$, 5 mM DTT, 1 mM PSMF, 10% (v/v) ethylene glycol (pH 7.5), 1 mM EDTA and 1% Polyclar), sonicated and centrifuged at 10,000 x g. The supernatant thus obtained was kept on ice and the pellet was treated with 60 µl of 1 M NaOH and centrifuged at 10,000 x g. The supernatants were used to quantify protein levels using a Bio-Rad DC protein assay kit.

Seed sucrose content analysis

For sucrose extraction, sets of 50 seeds were homogenized in 500 µl of 90% (v/v) ethanol, left at 70^{o}C for 90 min and centrifuged at 13,000 x g for 10 min. Sucrose content from the supernatants was determined by HPLC with pulsed amperometric detection on a DX-500 Dionex system by gradient separation with a CarboPac 10 column according to the application method suggested by the supplier (100 mM NaOH/100 mM sodium acetate to 100 mM NaOH/500 mM sodium acetate in 40 min).

Leaf starch content analysis

Fully expanded source leaves of plants were harvested at the end of the light period, freeze-clamped and ground to a fine powder in liquid nitrogen with a pestle and mortar. Starch was measured by using an amyloglucosidase–based test kit (Boehringer Mannheim, Germany).

Native gel PGI activity assays

PGI zymograms were acquired as described by Bahaji et al. (2015). Briefly, protein extracts of WT, *pgi1-2, promPGI1:PGI1* and *35S:PGI1* seeds collected 15 days after flowering were loaded onto a 7.5% (w/v) polyacrylamide gel. After electrophoresis, the gels were stained by incubating in darkness at room temperature with 0.1 M Tris-HCl (pH 8.0), 5 mM F6P, 1 mM NAD^{+}, 4 mM $MgCl_2$, 0.2 mM methylthiazolyldiphenyl-

517 tetrazolium bromide (Sigma M5655), 0.25 mM phenazine methosulfate (Sigma P9625)
518 and 1 U/mL of G6P dehydrogenase from *Leuconostoc mesenteroides* (Sigma G8404).
519
520 **Quantitative analysis of endogenous GAs**
521 GA samples were prepared and analyzed as described by Urbanová et al. (2013), with
522 some modifications. Briefly, freeze-dried plant tissue samples (5-10 mg) were ground to
523 a fine consistency using 3-mm zirconium oxide beads (Retsch GmbH & Co. KG, Haan,
524 Germany) and a MM 301 mill (Retsch GmbH & Co. KG, Haan, Germany) vibrating at 30
525 Hz for 3 min, with 1 mL of ice-cold 80% acetonitrile containing 5% formic acid as
526 extraction solution. The samples were then extracted overnight at 4 °C using a Stuart SB3
527 benchtop laboratory rotator (Bibby Scientific Ltd., Staffordshire, UK) after adding 17
528 internal GAs standards ($[^2H_2]GA_1$, $[^2H_2]GA_3$, $[^2H_2]GA_4$, $[^2H_2]GA_5$, $[^2H_2]GA_6$, $[^2H_2]GA_7$,
529 $[^2H_2]GA_8$, $[^2H_2]GA_9$, $[^2H_2]GA_{15}$, $[^2H_2]GA_{19}$, $[^2H_2]GA_{20}$, $[^2H_2]GA_{24}$, $[^2H_2]GA_{29}$,
530 $[^2H_2]GA_{34}$, $[^2H_2]GA_{44}$, $[^2H_2]GA_{51}$ and $[^2H_2]GA_{53}$; purchased from OlChemIm, Czech
531 Republic). The homogenates were centrifuged at 36,670 *g* and 4°C for 10 min, and the
532 corresponding supernatants were further purified using reversed-phase and mixed mode
533 SPE cartridges (Waters, Milford, MA, USA) and analyzed by ultra-high performance
534 chromatography-tandem mass spectrometry (UHPLC-MS/MS; Micromass, Manchester,
535 UK). GAs were detected using the multiple-reaction monitoring mode of the transition of
536 the ion $[M–H]^-$ to the appropriate product ion. Masslynx 4.1 software (Waters, Milford,
537 MA, USA) was used to analyze the data, and the standard isotope dilution method
538 (Rittenberg and Foster, 1940) was used to quantify the GAs.
539
540 **Statistical analysis**
541 The data presented are the means (± SE) from at least three independent experiments,
542 with 3-5 biological replicates for each experiment. The significance of differences
543 between control and transgenic lines was statistically evaluated with Student's t-test using
544 SPSS software. Differences were considered significant if $P<0.05$. In GA analyses,
545 significance was determined by one-way univariate analysis of variance (ANOVA) for
546 parametric data and Kruskal Wallis tests for non-parametric data, using open source R

2.15.1 software (http://cran.r-project.org/). Tukey's honest significant difference (HSD) post hoc tests were applied for multiple comparisons after ANOVA.

Accession numbers

Sequence data from the article can be found in the GenBank/EMBL libraries under accession numbers PGI1 (At4g24620, PKK4 (At5g61580), PFK5 (At2g22480), GA2ox1 (At1g78440), GA2ox2 (At1g30040), GA2ox3 (At2g34555), GA2ox4 (At1g47990), GA2ox6 (At1g02400), GA2ox7 (At1g50960), GA2ox8 (At4g21200), GA3ox1 (At1g15550), GA3ox2 (At1g80340), GA3ox3 (At4g21690), GA3ox4 (At1g80330), GA20ox1 (At4g25420), GA20ox2 (At5g51810), GA20ox3 (At5g07200), GA20ox4 (At1g60980), and GA20ox5 (At1g44090).

SUPPLEMENTAL DATA

Supplemental Figure 1: Starch content in mature leaves of Ws-2, *pgi1-2* and *promPGI1:PGI1* plants.

Supplemental Figure 2: Expression levels of different *GA2ox, GA3ox and GA20ox* genes in WT (Ws-2) and *pgi1-2* shoots.

Supplemental Figure 3: Embryo development in WT (Ws-2) and *pgi1-2* embryos at different developmental stages.

Supplemental Figure 4: Time-course of sucrose content in developing Ws-2 and *pgi1-2* seeds.

Supplemental Figure 5: Confirmation of the knock-out status of the *pfk4 pfk5* mutant**.**

Supplemental Figure 6: Stages in construction of the promPGI1:GUS, 35S:PGI1 and promPGI1:PGI1 plasmids used to produce *promPGI1:GUS-, 35S:PGI1-* and *promPGI1:PGI1-* expressing plants.

Supplemental Figure 7: Stages in construction of the 35S:PFK4, 35S:PFK5 and 35S:PFK5* plasmids used for transient expression in *N. benthamiana* leaves.

Supplemental Table 1: Primers used for PCR screening of the *pfk4 pfk5* mutant.

Supplemental Table 2: Primers used to produce the promPGI1:GUS, promPGI1:PGI1 35S:PGI1, 35S:PFK4, 35S:PFK5 and 35S:PFK5* plasmids.

Supplemental Table 3: Primers used in qRT-PCR analyses.

Supplemental Table 4: ANOVA table.

ACKNOWLEDGEMENTS

We thank Francisco Carreto-Cano (Institute of Agrobiotechnology of Navarra) for technical support. We also thank Dr. T. Werner (Freie Universität Berlin, Germany), R.E. Häusler (University of Cologne, Germany) and Dr. Peter Hedden (Rothhamsted Research, UK) who very kindly provided us the 35S:AtCKX1*, pgi1-2* and *ga20ox1 ga20ox2* mutants, respectively. This work was partially supported by the Comisión Interministerial de Ciencia y Tecnología and Fondo Europeo de Desarrollo Regional (Spain) (grant numbers BIO2013-49125-C2-1-P and BIO2016-78747-P), the Ministry of Education, Youth and Sports of the Czech Republic (grant LO1204 from the National Program of Sustainability I), the Government of Navarra (ref. P1004 PROMEBIO), the Università degli Studi di Milano (UNIMI-RTD-A, Linea2-DBS 2017-2018) and the H2020-MSCA-RISE project (ExpoSeed GA-691109).

AUTHOR CONTRIBUTIONS

A B, G A, I E, AM S-L, FJ M, N DD, L S, K D and J P-R designed the experiments and analyzed the data; A B, G A, I E, S GA, RJ B, MC S, D T, E C, MA M and E B-F performed most of the experiments; A B, I E, K D and J P-R supervised the experiments; A B, FJ M and J P-R wrote the article with contributions from all the authors; J P-R conceived the project and research plans.

609

610 **REFERENCES**

611 Bahaji, A. et al. (2015). Plastidic phosphoglucose isomerase is an important determinant
612 of starch accumulation in mesophyll cells, growth, photosynthetic capacity, and
613 biosynthesis of plastidic cytokinins in *Arabidopsis*. PLoS One 10: e0119641.
614 doi:10.1371/journal.pone.0119641.

615 Barker, R. (2011) Gibberellin biosynthesis and signalling in *Arabidopsis* root growth.
616 Ph.D. Thesis, University of Nottingham, Nottingham, U.K.

617 Bartrina, I., Otto, E., Strnad, M., Werner, T., and Schmülling, T. (2011). Cytokinin
618 regulates the activity of reproductive meristems, flower organ size, ovule formation,
619 and thus seed yield in *Arabidopsis thaliana*. Plant Cell 23: 69–80.

620 Baud, S., Dubreucq, B., Miquel, M., Rochat, C., and Lepiniec, L. (2008). Storage reserve
621 accumulation in *Arabidopsis*: metabolic and developmental control of seed filling.
622 Arabidopsis Book. doi:10.1199/tab.0113.

623 Baud, S., Wuillème, S., Dubreucq, B., de Almeida, A., Vuagnat, C., Lepiniec, L., Miquel,
624 M., and Rochat, C. (2007) Function of plastidial pyruvate kinases in seeds of
625 *Arabidopsis thaliana.* Plant J. 52: 405-419.

626 Bhargava, A., Clabaugh, I., To, J.P., Maxwell, B.B., Chiang, Y-H., Schaller, G.E.,
627 Loraine, A., and Kieber, J.J. (2013) Identification of cytokinin-responsive genes using
628 microarray meta-analysis and RNA-seq in Arabidopsis. Plant Physiol. 162: 272-294.

629 Brenner, W.G., and Schmülling, T. (2015) Summarizing and exploring data of a decade
630 of cytokinin-related transcriptomics. Frontiers Plant Sci. doi:10.3389/fpls.2015.00029.

631 Cernac, A., Andre, C., Hoffmann-Benning, S., and Benning, C. (2006). WRI1 is required
632 for seed germination and seedling establishment. Plant Physiol. 141: 745-757.

633 Chen, L.-Q., Lin, I.W., Qu, X.-Q., Sosso, D., McFarlane, H.E., Londoño, A., Samuels,
634 A.L., and Frommer, W.B. (2015). A cascade of sequentially expressed sucrose
635 transporters in the seed coat and endosperm provides nutrition for the Arabidopsis
636 embryo. Plant Cell 27: 607-619.

637 Chen, M., Du, X., Zhu, Y., Wang, Z., Hua, S., Li, Z., Guo, W., Zhang, G., Peng, J., and
638 Jiang, L. (2012a) *Seed Fatty Acid Reducer* acts downstream of gibberellin signalling
639 pathway to lower seed fatty acid storage in *Arabidopsis.* Plant Cell Environ. 35:

2155-2169.

Chen, M., Wang, Z., Zhu, Y., Li, Z., Hussain, N., Xuan, L., Guo, W., Zhang, G., and Jiang, L. (2012b) The effect of *TRANSPARENT TESTA2* on seed fatty acid biosynthesis and tolerance to environmental stresses during young seedling establishment in Arabidopsis. Plant Physiol. 160: 1023-1036.

Chen, M., Xuan, L., Wang, Z., Zhou, L., Li, Z., Du, X., Ali, E., Zhang, G., and Jiang, L. (2014) TRANSPARENT TESTA8 inhibits seed fatty acid accumulation by targeting several seed development regulators in Arabidopsis. Plant Physiol. 165: 905-916.

Clough, S.J. and Bent, A.F. (1998). Floral dip: A simplified method for Agrobacterium-mediated transformation of *Arabidopsis thaliana*. Plant J. 16: 735-743.

D'Aloia, M., Bonhomme, D., Bouché, F., Tamseddak, K., Ormenese, S., Torti, S., Coupland, G., and Périlleux, C. (2011). Cytokinin promotes flowering of *Arabidopsis* via transcriptional activation of the FT paralogue TSF. Plant J. 65: 972-979.

Eastmond, P.J. and Rawsthorne, S. (1998). Comparison of the metabolic properties of plastids isolated from developing leaves or embryos of *Brassica napus* L. J. Exp. Bot. 49: 1105-1111.

Eastmond, P.J. and Rawsthorne, S. (2000). Coordinate changes in carbon partitioning and plastidial metabolism during the development of oilseed rape embryos. Plant Physiol. 122: 767-774.

Fleet, C.M., and Sun, T-P. (2005). A DELLAcate balance: The role of gibberellin in plant morphogenesis. Curr. Opin. Plant Biol. 8: 77-85.

Focks, N., and Benning, C. (1998). *wrinkled1*: A novel, low-seed-oil mutant of *Arabidopsis* with a deficiency in the seed-specific regulation of carbohydrate metabolism. Plant Physiol. 118: 91-101.

Foyer, C.H., and Noctor, G. (2005) Redox homeostasis and antioxidant signaling: a metabolic interface between stress perception and physiological responses. Plant Cell 17: 1866-1875.

Girke, T., Todd, J., Ruuska, S., White, J., Benning, C., and Ohlrogge, J. (2000). Microarray analysis of developing Arabidopsis seeds. Plant Physiol. 124: 1570-1581.

671 Guo, L., Ma, F., Wei, F., Fanella, B., Allen, D.K., and Wang, X. (2014). Cytosolic
672 phosphorylating glyceraldehyde-3-phosphate dehydrogenases affect *Arabidopsis*
673 cellular metabolism and promote seed oil accumulation. Plant Cell 26: 3023-3035.
674 Hayashi, M., Toriyama, K., Kondo, M., and Nishimura, M. (1998). 2,4-
675 dichlorophenoxybutyric acid-resistant mutants of *Arabidopsis* have defects in
676 glyoxysomal fatty acid β-oxidation. Plant Cell 10: 183-195.
677 Hedden, P., and Thomas, S.G. (2012) Gibberellin biosynthesis and its regulation.
678 Biochem. J 444: 11-125.
679 Hutchings, D., Rawsthorne, S., and Emes, M.J. (2005). Fatty acid synthesis and the
680 oxidative pentose phosphate pathway in developing embryos of oilseed rape
681 (*Brassica napus* L.). J. Exp. Bot. 56: 577-585.
682 Jefferson, R., Kavanagh, T., and Bevan, M. (1987). GUS fusion: β-glucuronidase as a
683 sensitive and versatile gene fusion marker in higher plants. Embo J. 6: 3901-3907.
684 Jofuku, K.D., Omidyar, P.K., Gee, Z., and Okamuro, J.K. (2005) Control of seed mass
685 and seed yield by the floral homeotic gene *APETALA2.* Proc. Natl. Acad. Sci. USA
686 102: 3117-3122.
687 Kang, F., and Rawsthorne, S. (1996). Metabolism of glucose-6-phosphate and utilization
688 of multiple metabolites for fatty acid synthesis by plastids from developing oilseed
689 rape embryos. Planta 199: 321-327.
690 Kiba, T., Naitou, T., Koizumi, N., Yamashino, T., Sakakibara, H., and Mizuno, T. (2005)
691 Combinatorial microarray analysis revealing *Arabidopsis* genes implicated in
692 cytokinin responses through the His-Asp phosphorelay circuitry. Plant Cell Physiol.
693 46: 339-355.
694 Knappe, S., Löttgert, T., Schneider, A., Voll, L., Flügge, U-I., and Fischer, K. (2003).
695 Characterization of two functional *phosphoenolpyruvate/phosphate translocator*
696 (*PPT*) genes in *Arabidopsis-AtPTT1* may be involved in the provision of signals for
697 correct mesophyll development. Plant J. 36: 411-420.
698 Lee, E-J., Oh, M., Hwang, J-U., Li-Beisson, Y., Nishida, I., and Lee Y. (2017) Seed-
699 specific overexpression of the pyruvate transporter *BASS2* increases oil content in
700 *Arabidopsis* seeds. Front. Plant Sci. 8: 58. doi: 10.3389/fpls.2017.000194
701 Lee, D.J., and Zeevaart, J.A.D. (2007) Regulation of gibberellin 20-oxidase1 expression

in spinach by photoperiod. Planta 226: 35-44.

Liu, P., Zhang, H., Wang, H., and Xia, Y. (2014) Identification of redox-sensitive cysteines in the Arabidosis proteome using OxiTRAQ, a quantitative redox proteomics method. Proteomics 14: 750-762.

Lonien, J., and Schwender, J. (2009) Analysis of metabolic flux phenotypes for two Arabidopsis mutants with severe impairment in seed storage lipid synthesis. Plant Physiol. 151: 1617-1634.

Magome, H., Yamaguchi, S., Hanada, A., Kamiya, Y. and Oda, K. (2004) *dwarf and delayed-flowering 1,* a novel *Arabidopsis* mutant deficient in gibberellin biosynthesis because of overexpression of a putative AP2 transcription factor. Plant J. 37: 720-729.

Meng, L., and Feldman, L. (2010). A rapid TRIzol-based two-step method DNA-free RNA extraction from *Arabidopsis* siliques and dry seeds. Biotechnol. J. 5: 183-186.

Mitchum, M.G., Yamaguchi, S., Hanada, A., Kuwahara, A., Yoshioka, Y., Kato, T., Tabata, S., Kamiya, Y., and Sun, T. (2006) Distinct and overlapping roles of two gibberellin 3-oxidases in Arabidopsis development. Plant J. 45: 804-818.

Miyawaki, K. Matsumoto-Kitano, M., and Kakimoto, T. (2004) Expression of cytokinin biosynthetic isopentenyltransferase genes in *Arabidopsis:* tissue specificity and regulation by auxin, cytokinin, and nitrate. Plant J. 37: 128-138.

Mustroph, A., Sonnewald, U., and Biemelt, S. (2007). Characterization of the ATP-dependent phosphofructokinase gene family from *Arabidopsis thaliana.* FEBS Lett. 581: 2401-2410.

Mutasa-Göttgens, E., and Hedden, P. (2009). Gibberellin as a factor in floral regulatory networks. J. Exp. Bot. 60: 1979-1989

Née, G., Zaffagnini, M., Trost, P., and Issakidis-Bourguet, E. (2009). Redox regulation of chloroplastic glucose-6-phosphate dehydrogenase: A new role for f-type thioredoxin. FEBS Lett. 583: 2827-2832.

Prabhakar, V. et al. (2010). Phosphoenolpyruvate provision to plastids is essential for gametophyte and sporophyte development in *Arabidopsis thaliana*. Plant Cell 22: 2594-2617.

Pokhilko, A., Bou-Torrent, J., Pulido, P., Rodríguez-Concepción, M., and Ebenhöh, O.

(2015) Mathematical modelling of the diurnal regulation of the MEP pathway in *Arabidopsis*. New Phytol. 206: 1075-1085.

Pulido, P., Perello, C., and Rodríguez-Concepción, M. (2012). New insights into plant isoprenoid metabolism. Molecular Plant 5: 964-967.

Reiser, J., Linka, N., Lemke, L., Jeblick, W., and Neuhaus, H.E. (2004). Molecular physiological analysis of the two plastidic ATP/ADP transporters from *Arabidopsis*. Plant Physiol. 136: 3524-3536.

Riefler, M., Novak, O., Strnad, M., and Schmülling, T. (2006). *Arabidopsis* cytokinin receptor mutants reveal functions in shoot growth, leaf senescence, seed size, germination, root development, and cytokinin metabolism. Plant Cell 18: 40-54.

Rieu, I., Eriksson, S., Powers, S.J., Gong, F., Friffiths, J. Woolley, L., Benlloch, R., Nilsson, O., Thomas, S.G., Hedden, P., and Phillips, A.L. (2008a) Genetic analysis reveals that C19-GA 2-oxidation is a major gibberellin inactivation pathway in Arabidopsis. Plant Cell 20: 2420-2436.

Rieu, I., Ruiz-Rivero, O., Fernández-García, N., Griffiths, J., Powers, S.J., Gong, F., Linhartova, T., Eriksson, S., Nilsson, O., Thomas, S.G., Phillips, A.L., and Hedden, P. (2008b) The gibberellin biosynthetic genes *AtGA20ox1* and *AtGA20ox2* act, partially redundantly, to promote growth and development throughout the Arabidopsis life cycle. Plant J. 53: 488-504.

Rittenberg, D., and Foster, G.L. (1940) A new procedure for quantitative analysis by isotope dilution, with application to the determination of amino acids and fatty acids. J. Biol. Chem. 133: 737-744.

Ruuska, S.A., Girke, T., Benning, C., and Ohlrogge, J. (2002). Contrapuntal networks of gene expression during *Arabidopsis* seed filling. Plant Cell 14: 1191-1206.

Sánchez-López, Á.M. et al. (2016) Arabidopsis responds to *Alternaria alternata* volatiles by triggering plastid phosphoglucose isomerase-independent mechanisms. Plant Physiol. 172: 1989-2001.

Schwender, J., Goffman, F., Ohlrogge, J.B., and Shachar-Hill, Y. (2004). Rubisco without the Calvin cycle improves the carbon efficiency of developing green seeds. Nature 432: 779-782.

Schwender, J., Ohlrogge, J.B., and Shachar-Hill, Y. (2003). A flux model of glycolysis

764 and the oxidative pentosephosphate pathway in developing *Brassica napus* embryos.
765 J. Biol. Chem. 278: 29442-29453.
766 Silverstone, A.L., Chang, C., Krol, E., and Sun, T. (1997) Developmental regulation of
767 the gibberellin biosynthetic gene *GA1* in *Arabidopsis thaliana.* Plant J. 12: 9-19.
768 Spíchal, L. (2012) Cytokinins-recent news and views of evolutionally old molecules.
769 Funct. Plant Biol. 39: 267-284.
770 Tsai, H.L., Lue, W.L., Lu, K.J., Hsieh, M.H., Wang, S.M., and Chen, J. (2009). Starch
771 synthesis in *Arabidopsis* is achieved by spatial cotranscription of core starch
772 metabolism genes. Plant Physiol 151: 1582–1595.
773 Urbanová, T., Tarkowská, D., Novák, O., Hedden, P., and Strnad, M. (2013) Analysis of
774 gibberellins as free acids by ultra performance liquid chromatography–tandem mass
775 spectrometry. Talanta 112: 85-94.
776 van Daele, I., Gonzalez, N., Vercauteren, I., de Smet, L., Inzé, D., Roldán-Ruiz, I., and
777 Vuylsteke, M. (2012) A comparative study of seed yield parameters in *Arabidopsis*
778 *thaliana* mutants and transgenics. Plant Biotechnol. J. 10: 488-500.
779 Ventriglia, T., Kuhn, M.L., Ruiz, M.T., Ribeiro-Pedro, M., Valverde, F., Ballicora, M.A.,
780 Preiss, J., and Romero, J.M. (2008) Two Arabidopsis ADP-glucose
781 pyrophosphorylase large subunits (APL1 and APL2) are catalytic. Plant Physiol.
782 148: 65-76.
783 Voinnet, O., Rivas, S., Mestre, P., and Baulcombe, D. (2003) An enhanced transient
784 expression system in plants based on suppression of gene silencing by the p19
785 protein of tomate bushi stunt virus. Plant J. 33: 949-956.
786 Werner, T., Motyka, V., Laucou, V., Smets, R., Van Onckelen, H., and Schmülling, T.
787 (2003). Cytokinin-deficient transgenic *Arabidopsis* plants show functions of
788 cytokinins in the regulation of shoot and root meristem activity. Plant Cell 15: 2532-
789 2550.
790 White, J.A., Todd, J., Newman, T., Focks, N., Girke, T., Martínez de Ilarduya, O.,
791 Jaworski, J.G., Ohlrogge, J.B., and Benning, C. (2000). A new set of Arabidopsis
792 expressed sequence tags from developing seeds. The metabolic pathway from
793 carbohydrates to seed oil. Plant Physiol. 124: 1582-1594.
794 Winter, D., Vinegar, B., Nahal, H., Ammar, R., Wilson, G.V., and Provart, N.J. (2007)

An "Electronic Fluorescent Pictograph" browser for exploring and analyzing large scale biological data sets. PLoS ONE 2: e718.

Yamaguchi, S. (2008) Gibberellin metabolism and its regulation. Annu. Rev. Plant Biol. 59: 225-251.

Yamaguchi, N., Winter, C.M., Wu, M-F., Yamaguchi, A., Seo, M., and Wagner, D. (2014) Gibberellin acts positively then negatively to control onset of flower formation in *Arabidopsis.* Science 34: 638-641.

Yin, Z., Balmant, K., Geng, S., Zhu, N., Zhang, T., Dufresne, C., Dai, S., and Che, S. (2017) Bicarbonate induced redox proteome changes in Arabidopsis suspension cells. Front. Plant Sci. 8: 58. doi: 10.3389/fpls.2017.00058

Yu, T.S., Lue, W.L., Wang, S.M., and Chen, J. (2000). Mutation of *Arabidopsis* plastid phosphoglucose isomerase affects leaf starch synthesis and floral initiation. Plant Physiol. 123: 319-326.

Table 1: Harvest parameters for WT (Ws-2 and Col-*0*), *pgi1-2, promPGI1:PGI1(1), 35S:PGI1* and *aps1* plants. Values are means ± SE obtained from four independent experiments using 10 plants in each experiment. The asterisks (*) indicate significant differences with respect to WT according to Student's t-tests (p<0.05).

Plant line	Number of elongated inflorescences per plant	Number of siliques per plant	Number of seeds per silique	Specific seed weight (μg seed^{-1})	Seed yield (mg plant^{-1})
Ws-2	29.5 ± 2.5	684.1 ± 14.7	48.2 ± 0.8	18.1 ± 0.8	596.8 ± 22.1
pgi1-2	15.3 ± 1.3*	457.3 ± 22.4*	47.2 ± 0.9	11.7 ± 0.4*	252.5 ± 7.3*
promPGI1: PGI1(1)	27.5 ± 1.9	682.4 ± 18.2	46.6 ± 1.3	18.0 ± 0.5	572.4 ± 9.8
35S:PGI1	28.6 ± 0.9	662.7 ± 21.5	47.3 ± 1.2	18.2 ± 0.6	570.4 ± 19.7
Col-*0*	30.6 ± 2.6	766.1 ± 40.8	57.2 ± 0.9	17.1 ± 1.0	749.3 ± 11.9
aps1	29.6 ± 3.0	761.6 ± 22.2	58.2 ± 0.9	17.6 ± 0.7	780.1 ± 19.9

819 **Table 2:** Number of inflorescences and siliques produced by WT and *pgi1-2* plants with
820 or without exogenous 100 μM BAP or GA_{4+7} treatment. Values are means ± SE obtained
821 from four independent experiments using 10 plants in each experiment. The asterisks (*)
822 indicate significant differences with respect to WT according to Student´s t-tests
823 (p<0.05).
824
825

Plant line	Number of elongated inflorescences per plant	Number of siliques per plant
Ws-2	29.5 ± 2.5	684.1 ± 14.7
pgi1-2	15.3 ± 1.3*	457.3 ± 22.4*
Ws-2 + GA	27.3 ± 1.5	729.1 ± 34.2
pgi1-2 + GA	27.1 ± 2.2	715.6 ± 74.1
Ws-2 + BAP	26.4 ± 1.8	657.3 ± 19.3
pgi1-2 + BAP	14.4 ± 1.2*	417.3 ± 26.4*

826

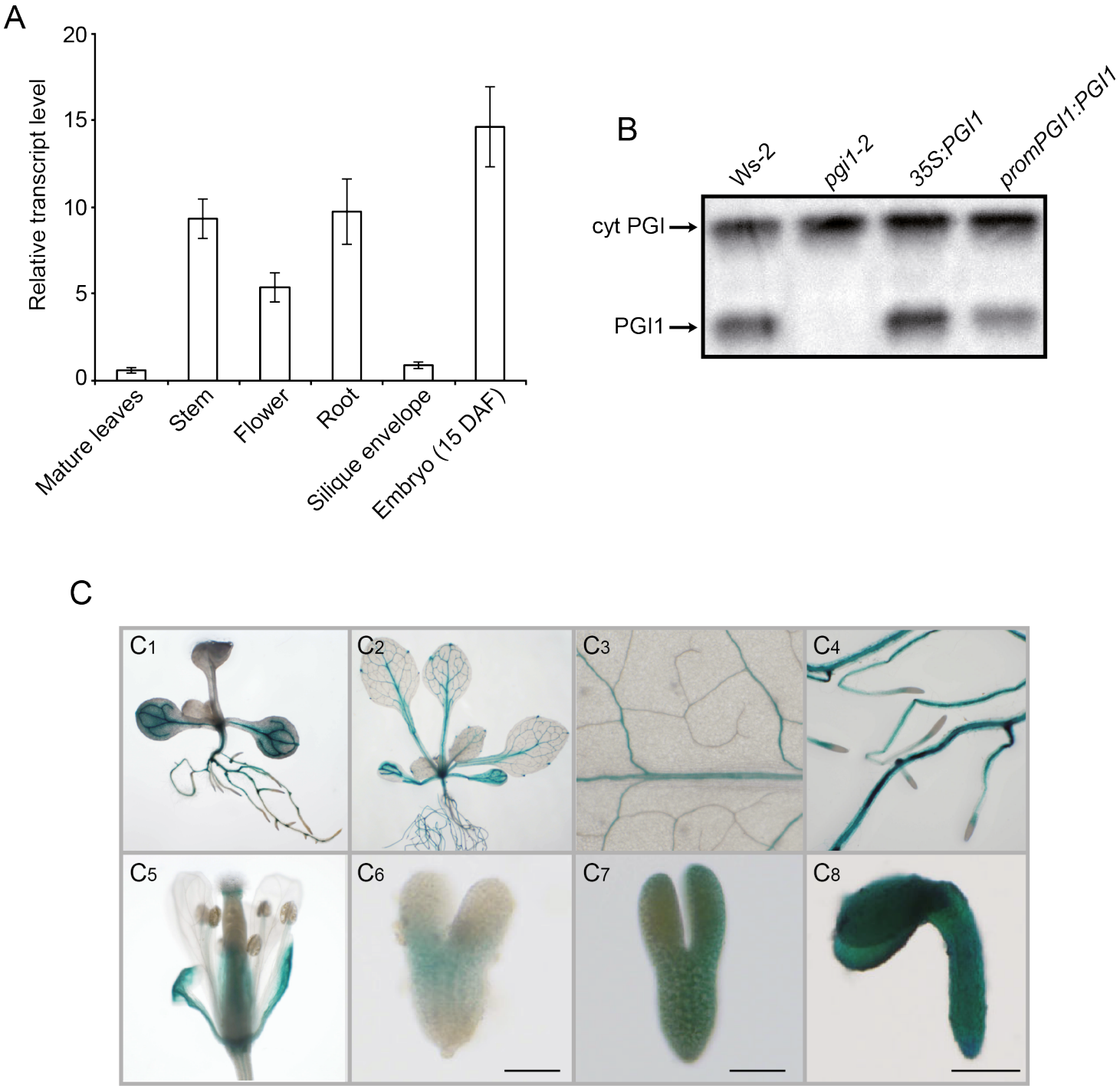

Figure 1. Expression pattern of *PGI1*. **(A)** qRT-PCR analysis of *PGI1* expression in indicated organs of Arabidopsis. Values represent the means ± SE of four biological replicates obtained from four independent experiments, each biological replicate being a pool of the indicated organs from four plants. **(B)** Zymogramic detection of PGI in proteins extracted from WT (Ws-2), *pgi1-2, promPGI1:PGI1* and *35S:PGI1* developing seeds. **(C)** Tissue-specific expression pattern of *PGI1* in transgenic *promPGI1:GUS* plants, as manifested by GUS histochemical staining of a young seedling **(C_1)**, a 3-week-old plant **(C_2)**, a magnified expanded leaf **(C_3)** and roots **(C_4)**, a flower **(C_5)**, and three stages of embryo development **($C_{6\text{-}8}$)**. **(C_6)** heart stage embryo, **(C_7)** embryo during transition from heart to torpedo stage, **(C_8)** mature embryo. DAF: Days after flowering.
Bars = 50 mm in **C_6** and **C_7**, 200 mm in **C_8**.

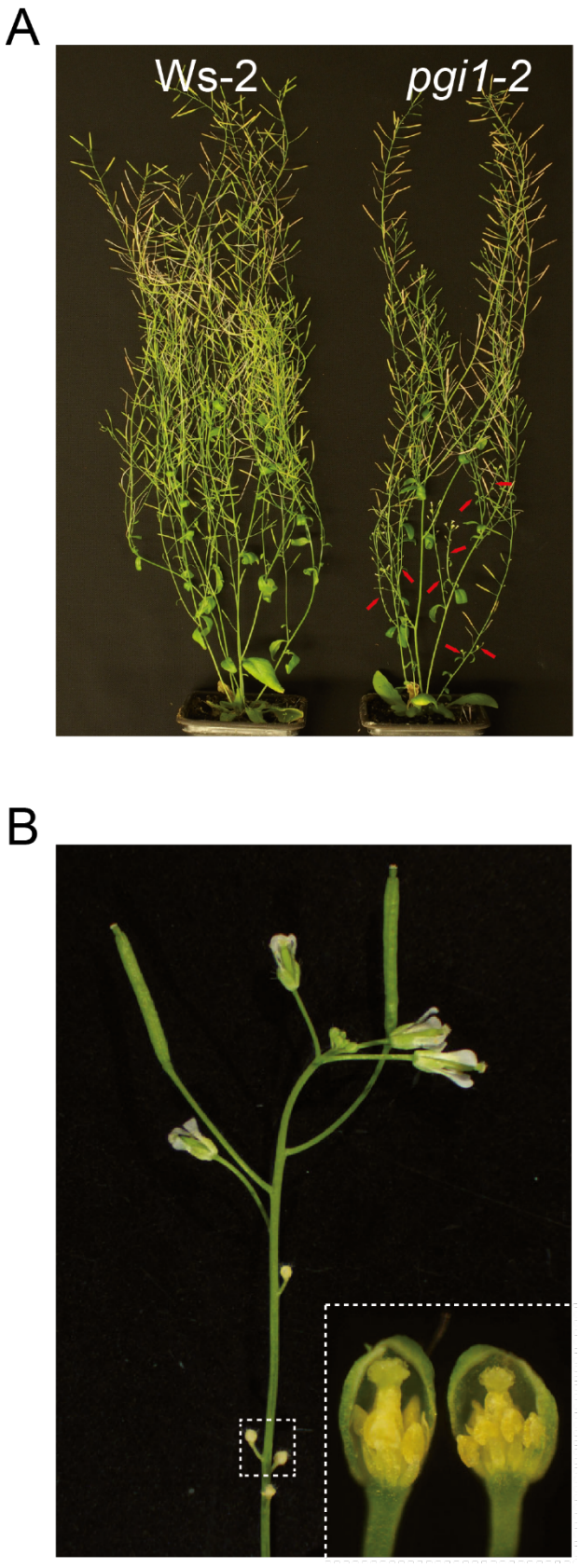

Figure 2: Knocking out *PGI1* reduces the number of elongated inflorescences and causes anther development arrest in the first flowers of inflorescences that do not elongate. **(A)** External phenotype of mature Ws-2 and *pgi1-2* plants. **(B)** External phenotype of a representative inflorescence that does not elongate in *pgi1-2* plants and morphology of two dissected early flowers from the same inflorescence. In “A”, red arrows indicate inflorescences that do not elongate in *pgi1-2* plants.

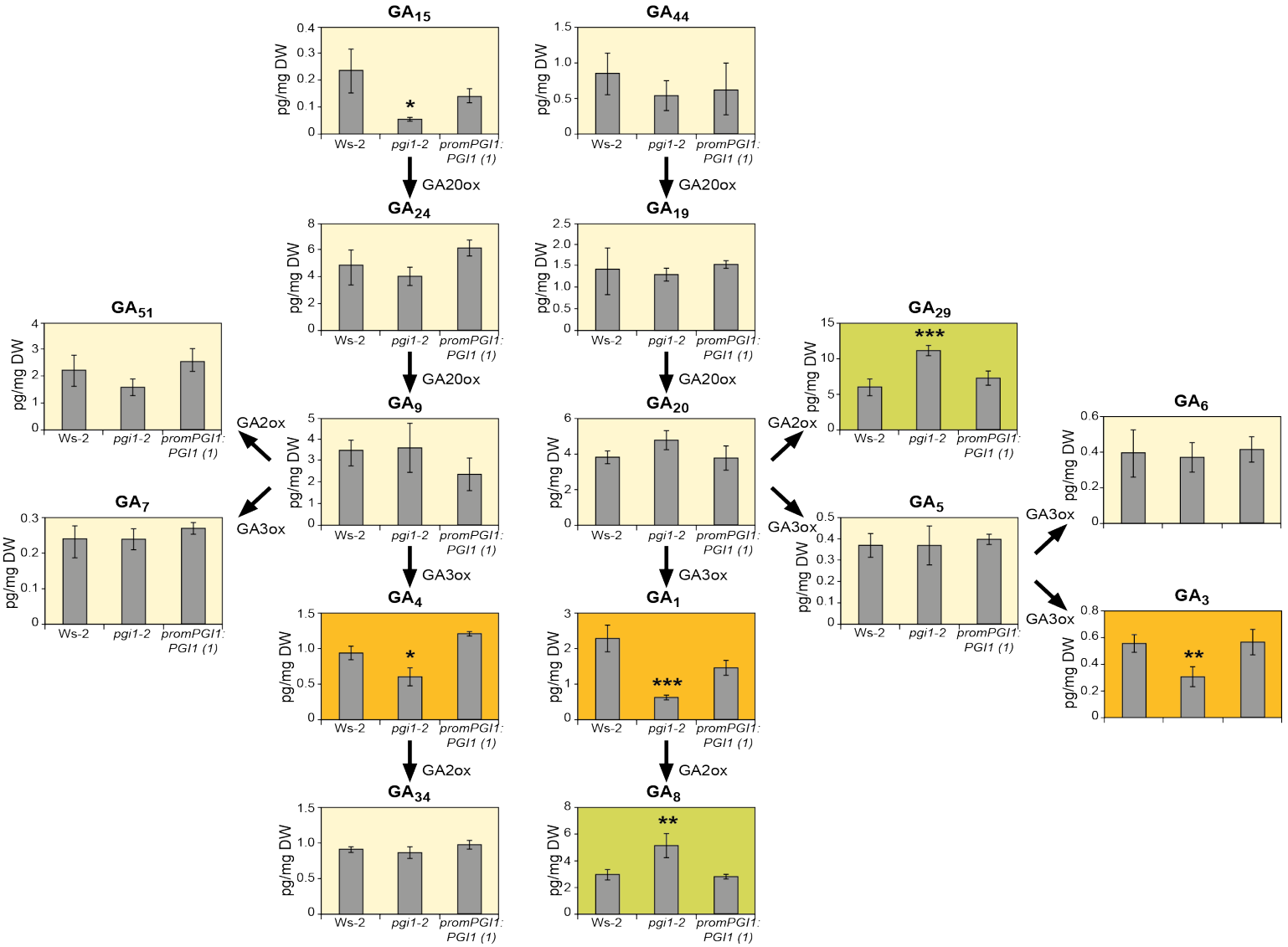

Figure 3. Knocking out *PGI1* decreases levels of bioactive GAs and increases levels of inactive GAs. The graphics show contents of indicated GAs (pg mg^{-1} DW) in shoots (20 days after sowing) of Ws-2 and *pgi1-2* plants, and *pgi1-2* plants transformed with *promPGI1:PGI1(1)*. Plants were harvested at the end of the light phase. Active GAs (significantly less abundant in *pgi1-2* plants than in Ws-2 plants) and inactive GAs (significantly more abundant in *pgi1-2* plants than in Ws-2 plants) are highlighted in orange and green, respectively. Values represent the means ± SE of two independent experiments, each consisting of four biological replicates corresponding to a pool of shoots from four plants. Asterisks indicate significant differences with respect to Ws-2 according to ANOVA (*P< 0.05; ** P <0.01; *** P <0.001).

.

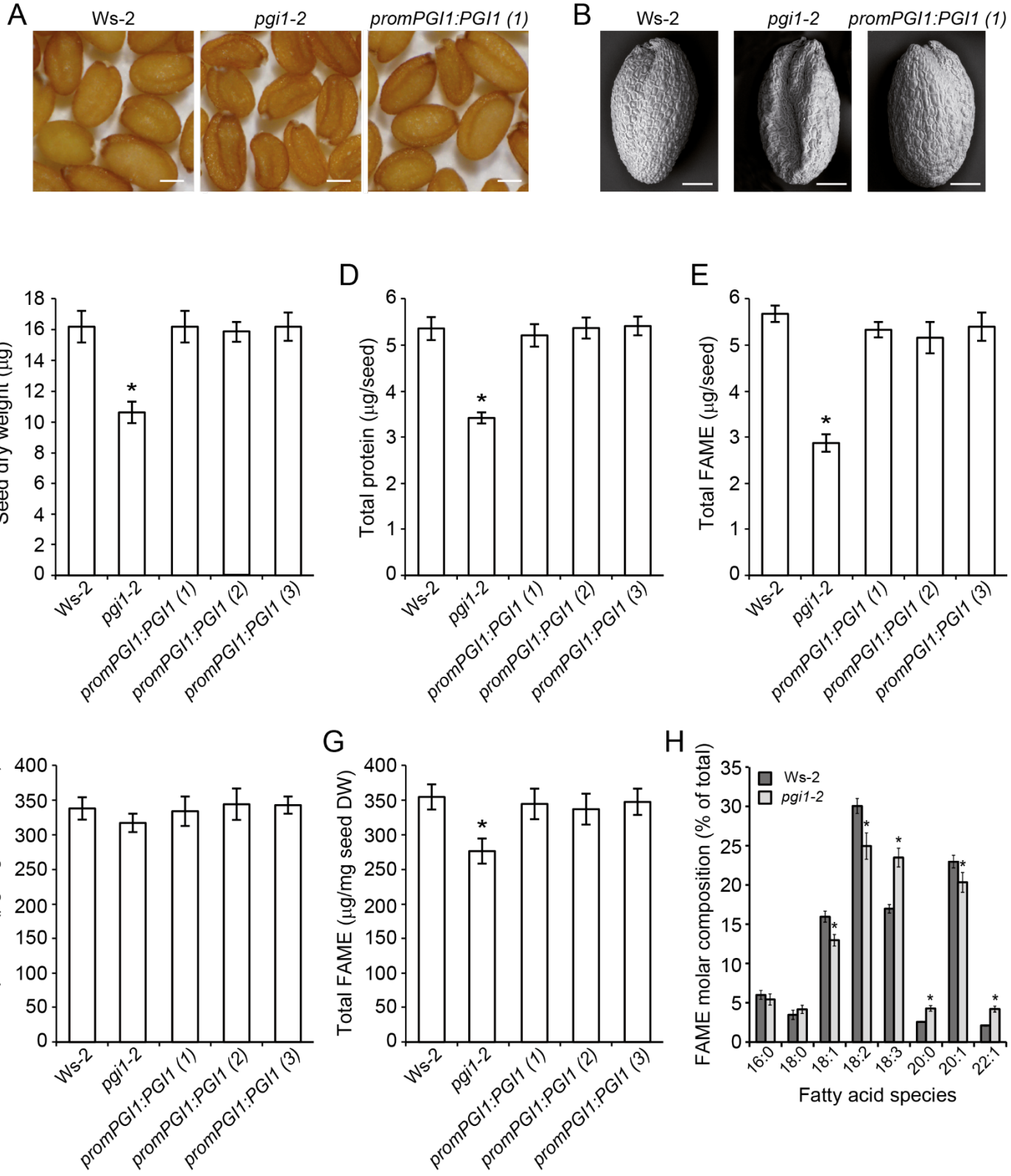

Figure 4. Protein and FA contents are diminished in *pgi1-2* seeds. **(A)** External phenotype and **(B)** scanning electron micrographs of seeds from WT (Ws-2) and *pgi1-2* plants, and one line of *pgi1-2* plants ectopically expressing *PGI1* under control of the *PGI1* promoter (*promPGI1:PGI1(1)*). **(C)** Seed dry weight, **(D)** total protein content per seed, **(E)** total FAME contents per seed, **(F)** total protein content on DW basis and **(G)** total FAMEs content on DW basis of dry seeds of WT, *pgi1-2* and three independent lines of *pgi1-2* plants ectopically expressing *PGI1* under control of the *PGI1* promoter (*promPGI1:PGI1(1-3)*). **(H)** FA profile of dry mature WT and *pgi1-2* seeds. Values in C, D, E, F, G and H represent the means ± SE of four biological replicates obtained from four independent experiments, each biological replicate being a pool of 300 seeds **(C)**, 200 seeds **(D, F)** or 20 seeds **(E, G, H)**. Asterisks indicate significant differences from WT seeds according to Student´s t-tests (p<0.05). Scale bars in A and B = 200 mm and 100 mm, respectively.

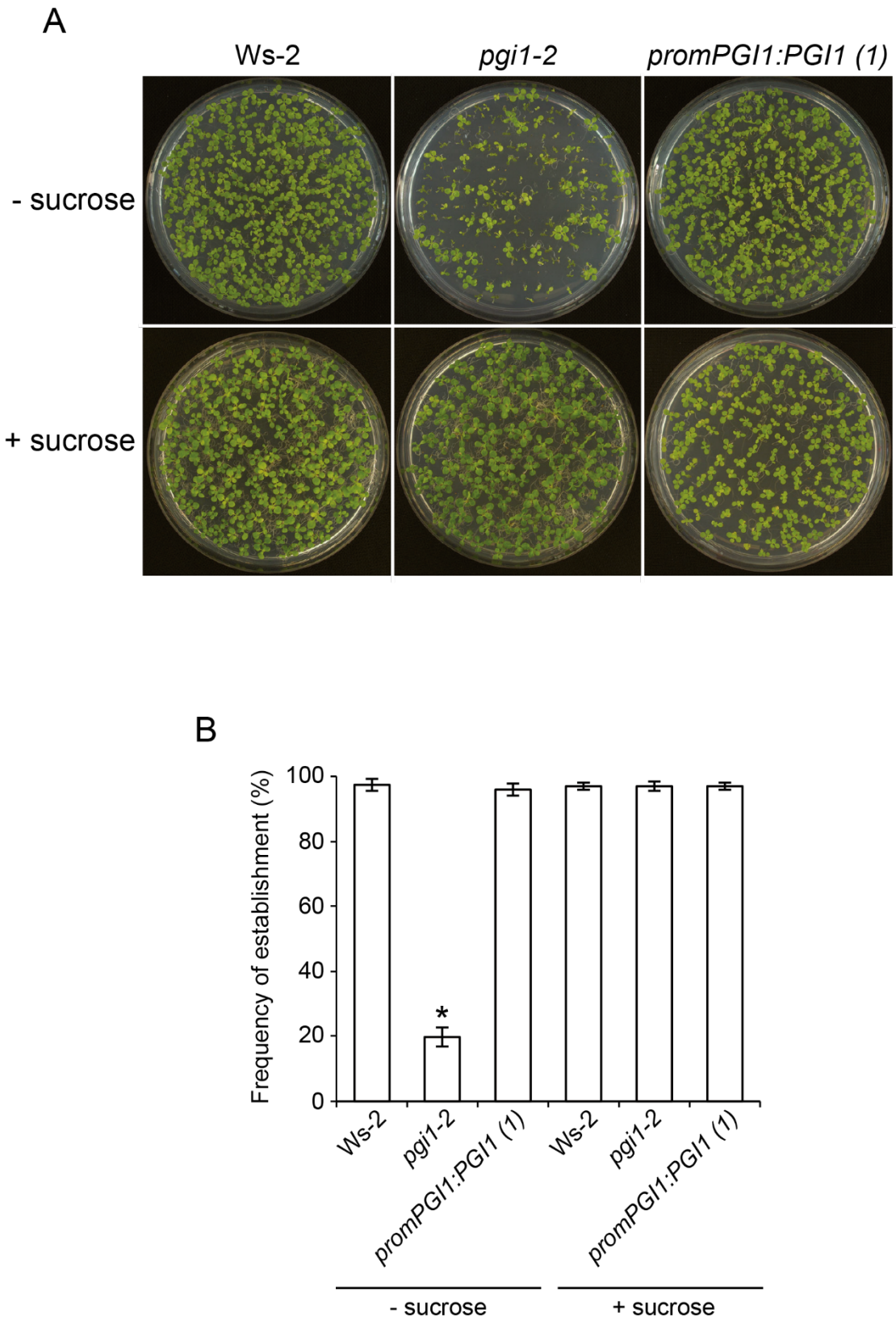

Figure 5. *pgi1-2* seedlings have reduced establishment rates. **(A)** Photographs and **(B)** establishment rates 12 days after sowing of WT (Ws-2), *pgi1-2* and *promPGI1:PGI1(1)* plants cultured in MS with or without sucrose supplementation. Values in B are means ± SE of four biological replicates obtained from four independent experiments, each biological replicate being approximately 100 seeds. The asterisk indicates significant differences in establishment rates between WT and *pgi1-2* plants according to Student´s t-tests (p<0.05).

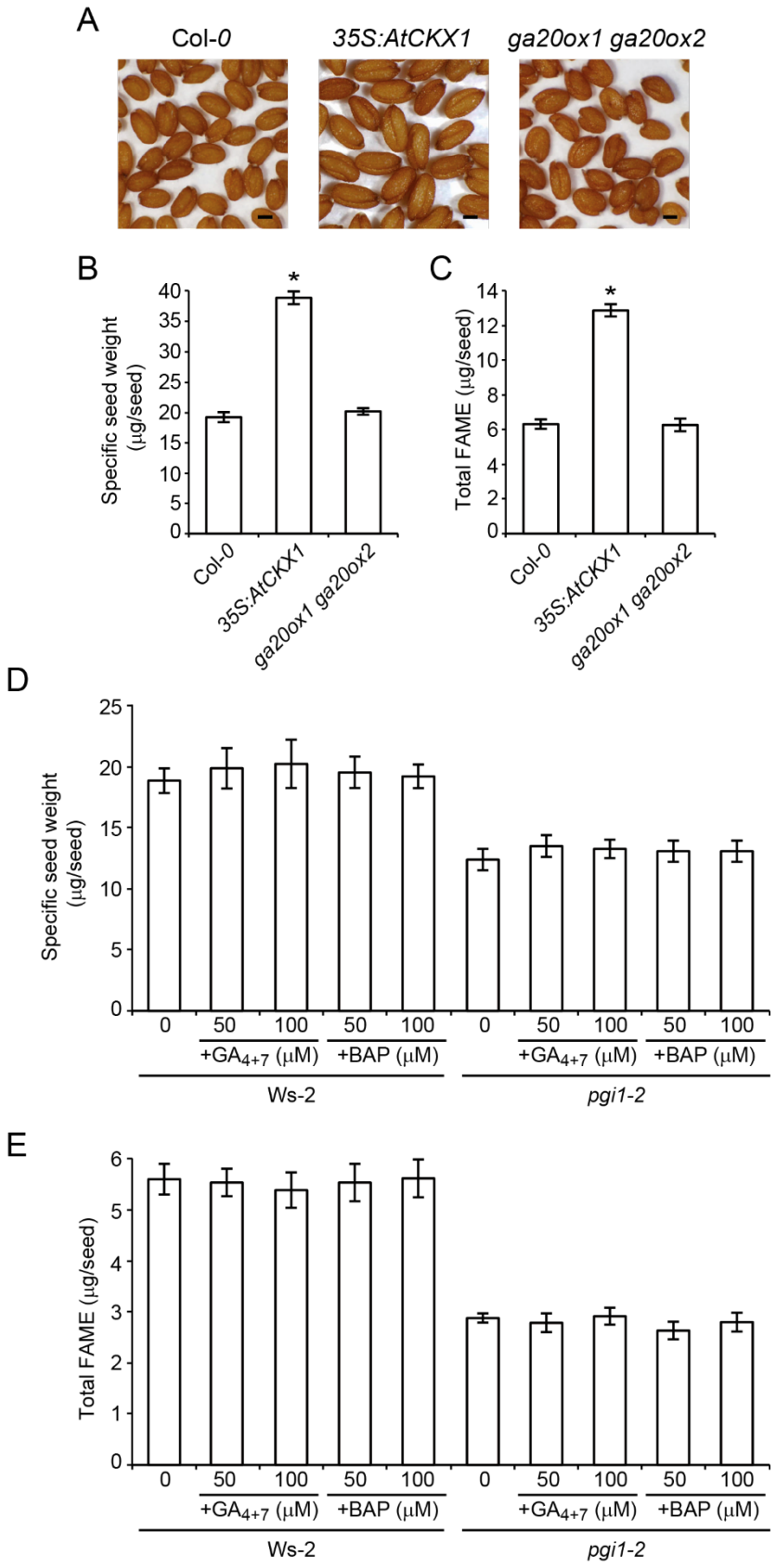

Figure 6: The low FA content phenotype of *pgi1-2* seeds is not due to reduced active CK or GA contents. **(A)** External phenotype, **(B)** specific weight and **(C)** total FAME contents of WT (Col-*0*), *35S:AtCKX1* and *ga20ox1 ga20ox2* dry seeds. **(D)** Specific weight and **(E)** total FAME contents of dry seeds of Ws-2 and *pgi1-2* plants following exogenous CK and GA_{4+7} application. Scale bar in A = 200 mm. Values in B, C, D and E, represent the means ± SE of four biological replicates obtained from three independent experiments, each biological replicate being a pool of 300 seeds **(B, D)** or 20 seeds **(C, E)**. In "B" and "C", asterisks indicate significant differences from WT seeds according to Student´s t-tests (p<0.05).

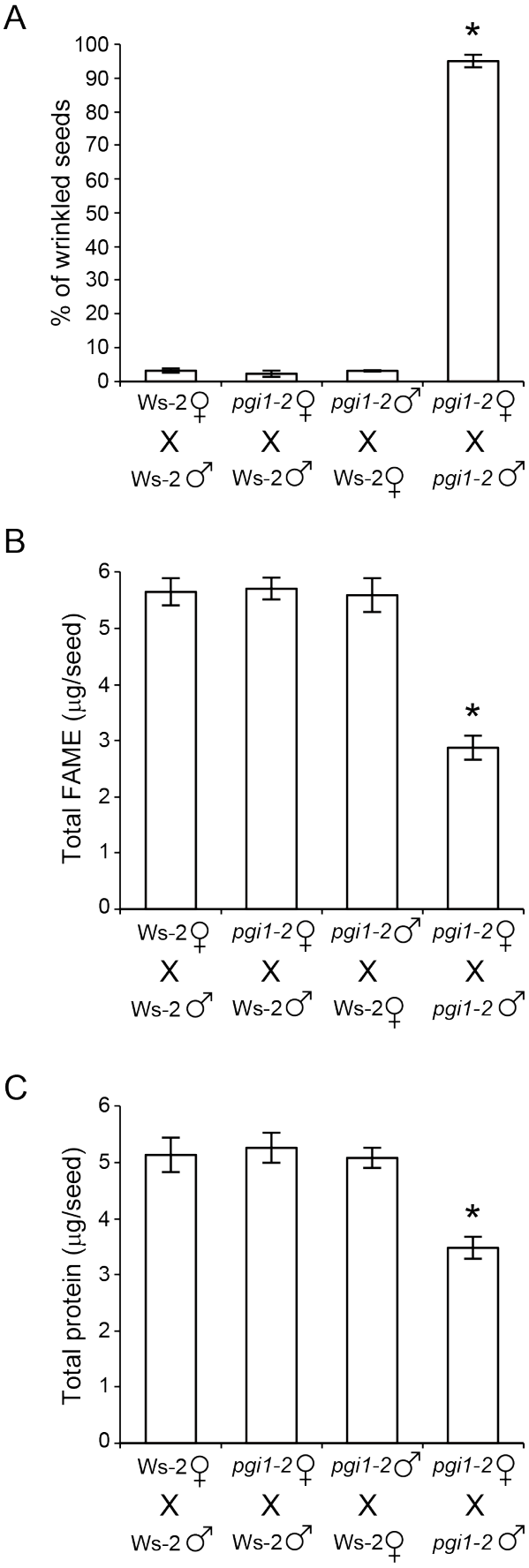

Figure 7. The phenotype of *pgi1-2* seeds is embryonically controlled. **(A)** Percentage of wrinkled seeds, **(B)** total FAME and **(C)** protein contents in the F1 progeny of indicated WT (Ws-2) and *pgi1-2* crosses. Values represent the means ± SE of three biological replicates obtained from three independent experiments, each biological replicate being a pool of 300 seeds **(A)**, 20 seeds **(B)** or 200 seeds **(C)**.

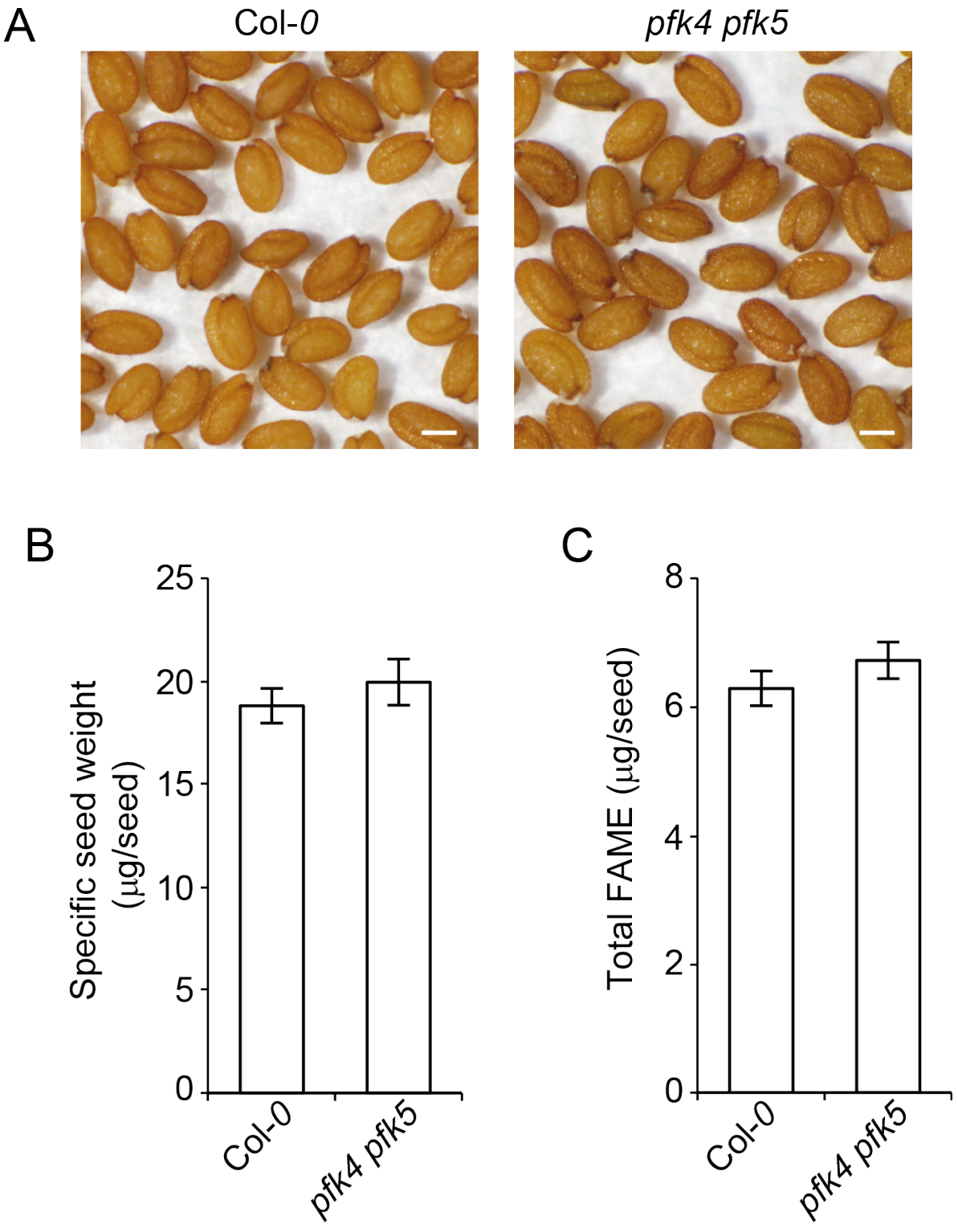

Figure 8: Plastidial PFK-mediated metabolism of F6P produced by PGI1 is not absolutely required for normal FA biosynthesis in Arabidopsis. **(A)** External phenotype, **(B)** specific weight and **(C)** total FAME contents of WT (Col-*0*) and *pfk4/pfk5* dry seeds. Scale bar in A = 200 mm. In "B" and "C", values represent the means ± SE of three biological replicates obtained from five independent experiments, each biological replicate being a pool of 300 seeds **(B)** or 20 seeds **(C)**.

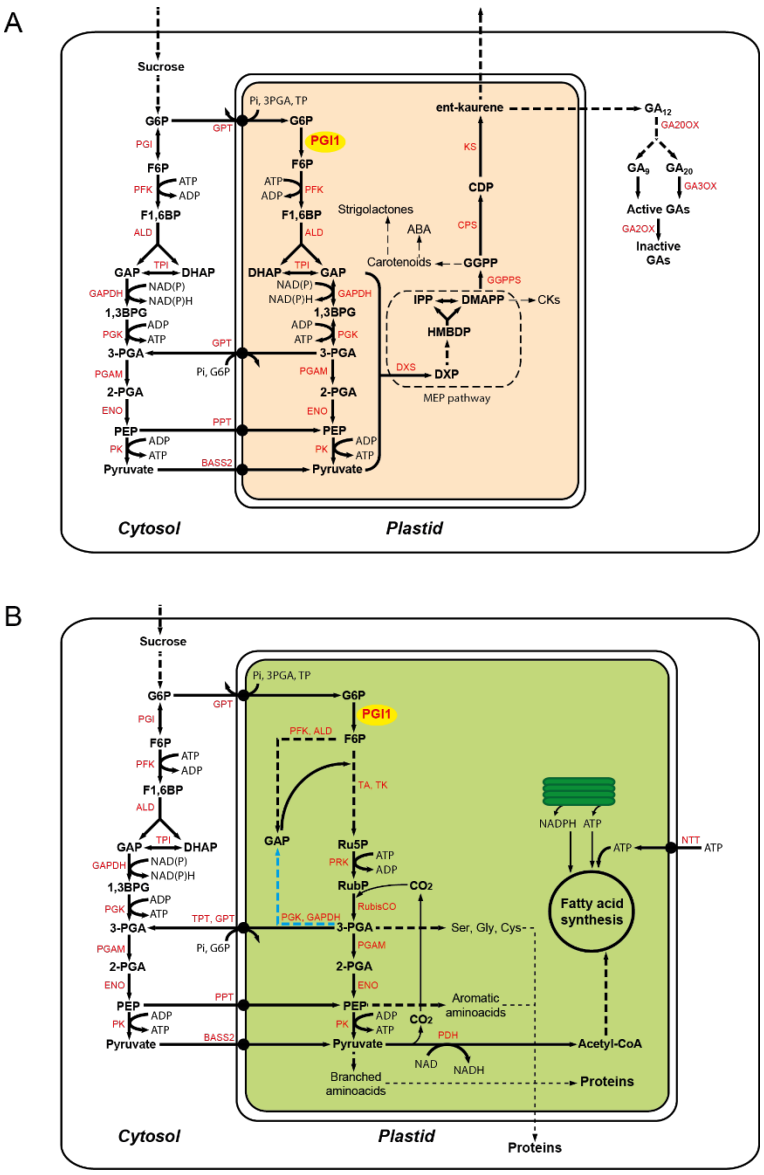

Figure 9. Suggested schemes for PGI1-mediated biosynthesis of **(A)** MEP-pathway isoprenoid derived CKs and GAs in cells of vascular tissues, and **(B)** FAs and proteins in mixotrophic maturing embryos of *Arabidopsis thaliana.* In both cases, cytosolic G6P can be glycolytically converted to PEP and pyruvate, which can enter plastids via the PPT and the BASS2 transporters, respectively. According to scheme **A**, some of the cytosolic G6P can be incorporated into plastids through the hexose-P transporter (GPT) and subsequently glycolytically converted to GAP and pyruvate. Plastidial GAP and pyruvate are then metabolized by 1-deoxy-D-xylulose 5-phosphate (DXP) synthase (DXS) to products that enter the MEP pathway and fuel synthesis of isoprenoid hormones (Pulido et al., 2012, Pokhilko et al., 2015). DMAPP can be converted to *ent*-kaurene in a three-steps process catalyzed by geranylgeranyl diphosphate (GGPP) synthase (GGPPS), CPS and ent-kaurene synthase (KS). *ent*-Kaurene can be then transported to other parts of the plant or oxidized to GA_{12}, which is converted to bioactive GA in the cytosol by GA20ox and GA3ox. DMAPP can also be converted to CKs (Spíchal, 2012). In heterotrophic cells lacking plastid-localized phosphoglyceromutase (PGAM), enolase (ENO) and the triose-P translocator (TPT), 3PGA produced in the plastid via PGI1 can be exported to the cytosol via GPT or other non-specific transporters then glycolytically converted into PEP and pyruvate, which can then enter plastids through the PPT and the BASS2 pyruvate transporter, respectively. According to scheme **B**, some of the cytosolic G6P can be incorporated into plastids through GPT and converted to 3PGA by the RubisCO shunt, which involves reactions of the early steps of glycolysis (PFK and aldolase), reactions of the non-oxidative pentose phosphate pathway, phosphoribulokinase (PRK) and RubisCO. In plants lacking plastidial PFK, part of the 3PGA generated can be converted to GAP necessary for Ru5P production by means of plastidial GAPDH and PGK (highlighted in blue). 3PGA can leave plastids via the TPT, the GPT or other non-specific transporters and glycolytically converted to PEP and pyruvate in the cytosol, which can enter plastids, as indicated above. Alternatively, and/or additionally, plastidial 3PGA can be converted to pyruvate in plastids. The ATP required for FA synthesis can be generated from photosynthesis and the PK reaction in the plastidial compartment, or obtained from the cytosol via the NTT transporter (Reiser et al., 2004). NADPH and NADH can be generated in plastids from the light photosynthetic and pyruvate dehydrogenase reactions, respectively. ALD: aldolase; TA: transaldolase; TK: transketolase; TPI: triose-phosphate isomerase; PDH: pyruvate dehydrogenase; HMBDP: (*E*)-4-Hydroxy-3-methyl-but-2-enyl diphosphate; IPP: isopentenyl diphosphate; CDP: *ent*-copalyl diphosphate. Enzymes are highlighted in red.

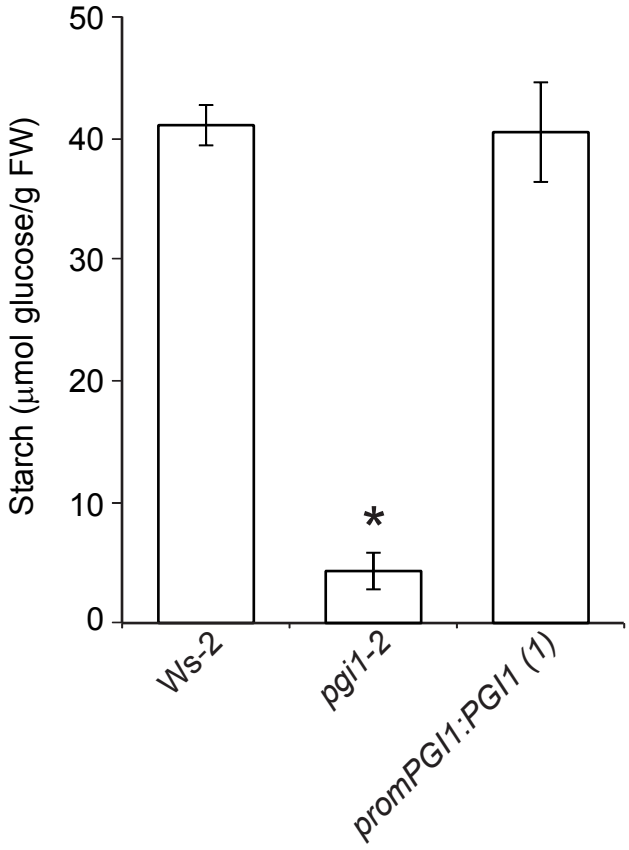

Supplemental Figure 1: Starch content in mature leaves of Ws-2, *pgi1-2* and *promPGI1:PGI1(1)*) plants. Values represent the means ± SE of four biological replicates obtained from four independent experiments, each biological replicate being a pool of mature leaves from four plants. Leaves were harvested after 12 h of illumination. The asterisk indicates significant differences from WT leaves according to Student´s t-tests ($p<0.05$) (**Supports Figure 1**).

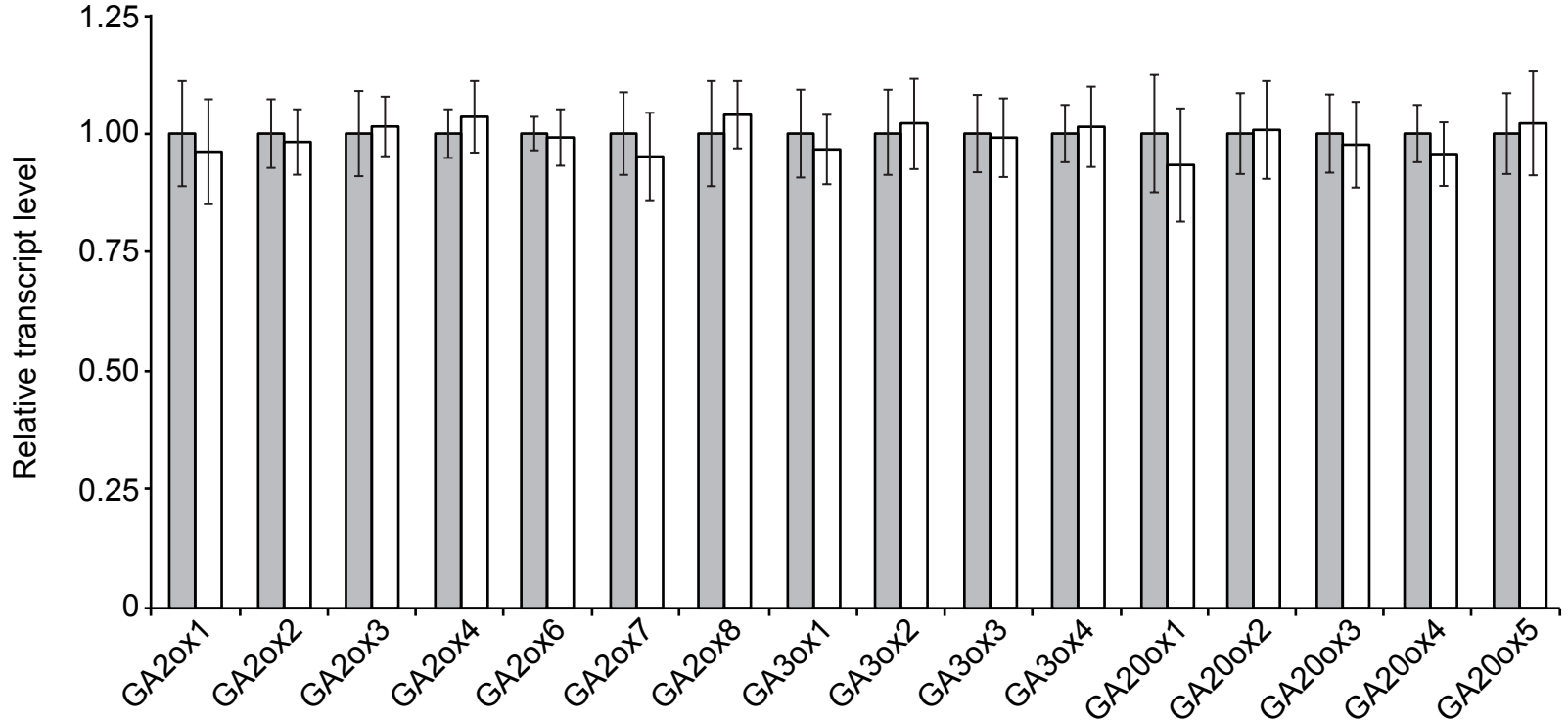

Supplemental Figure 2: Expression levels of different *GA2ox*, *GA3ox* and *GA20ox* genes in WT (Ws-2) and *pgi1-2* shoots (gray and white bars, respectively). mRNA levels are set to 1. Values represent the means ± SE of three independent experiments, each consisting of four biological replicates corresponding to a pool of four shoots. Leaves were harvested after 12 h of illumination (**Supports Figure 3**).

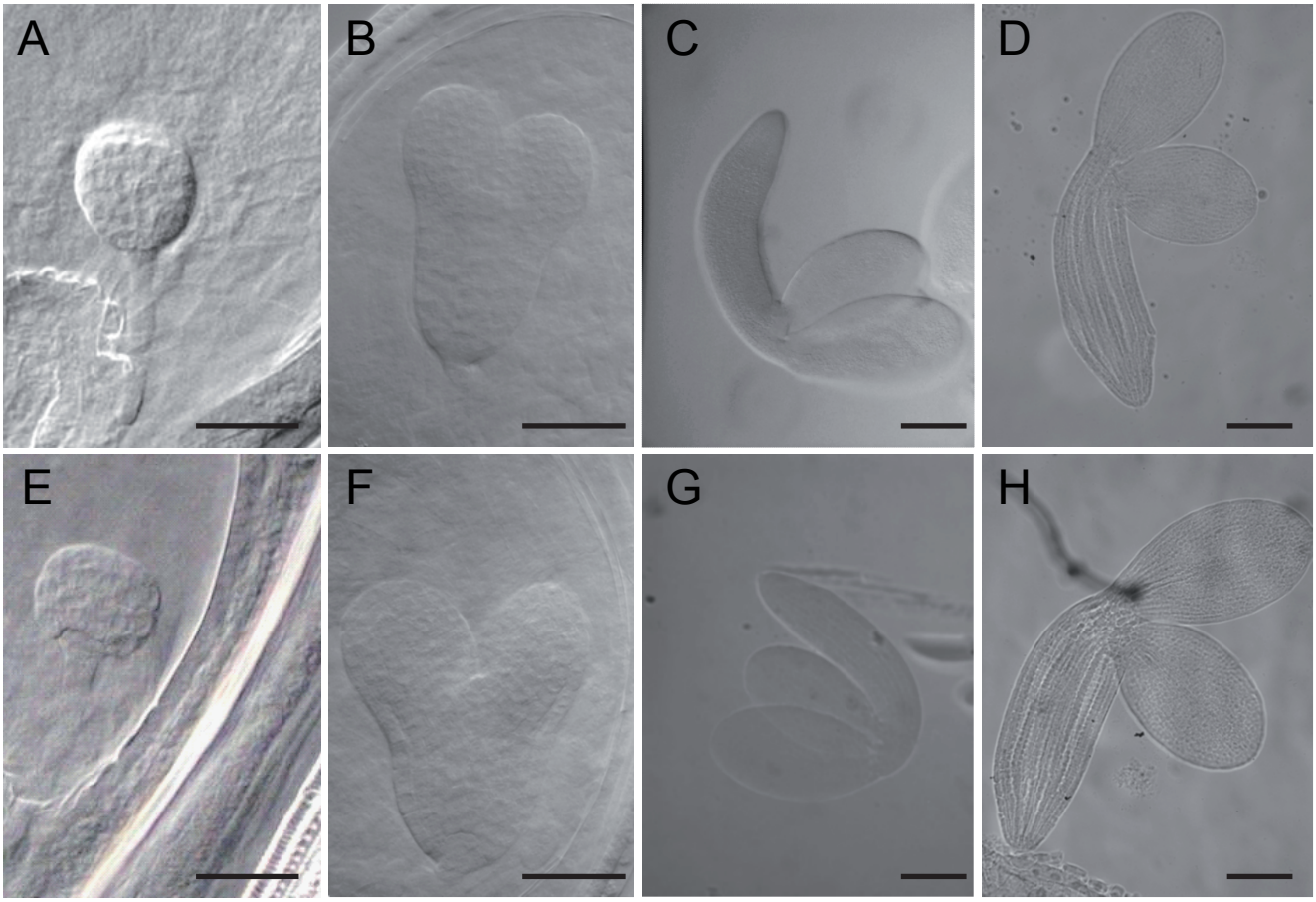

Supplemental Figure 3: Embryo development in WT (Ws-2) **(A–D)** and *pgi1-2* **(E–H)** embryos at: **A** and **E**, globular embryo stage; **B** and **F**, heart stage; **C** and **G**, mid-torpedo stage; **D** and **H**, mature embryo stage. Bars = 10 µm in **A** and **E**; 20 µm in **B-D** and **F-H** (**Supports Figure 4**).

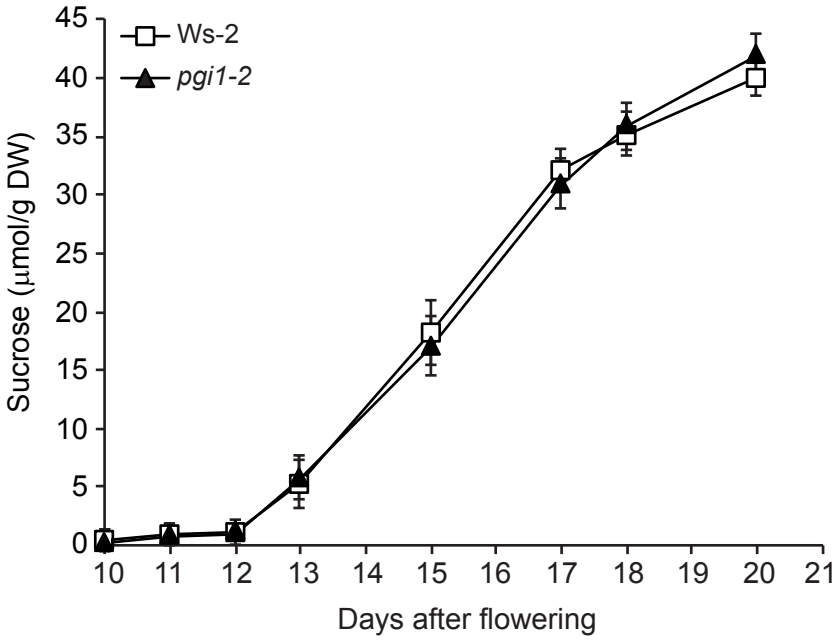

Supplemental Figure 4: Time-course of sucrose content in developing Ws-2 and *pgi1-2* seeds. Values represent the means ± SE of three biological replicates obtained from three independent experiments, each biological replicate being a pool of 50 seeds from four plants (**Supports Figure 4**).

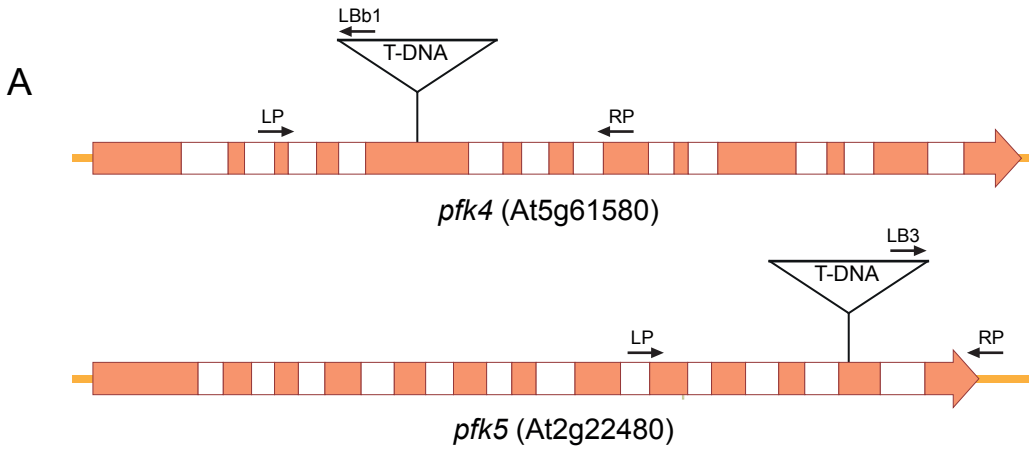

B

```
mdalsqaiss gisvpyknns sslvpshglt slilrksrsp vnpssrsrvs
vraseiqhsk tsassidlsd pdwklkyekd feqrfsiphi tdvlpdaeai
rstfclkmrs ptedfvggyp sdeewhgyin nndrvllkvi syssptsaga
ecldhdcswv eqwihragpr ekiyfrpeev kaaiitcggl cpglndvirh
ivitleiygv knivgipfgy rgfsdkdlte mplsrkvvqn ihlsggsllg
vsrggpsvse ivdsmeergi nmlfvlggng thaganaihn ecrkrkikva
vvgvpktidn dilhmdktfg fdtaveeaqr ainsayieah sayhgigvvk
lmgrnsgfia mqaslasgqv diclipevpf nlhgpngvlk hlkylietkg
savicvaega gqnflektna kdasgnavlg dfgvyiqqet kkyfkeistp
idvkyidpty miravranas dgilctvlgq navhgafagy sgitvgiint
hyaylpitev iaypksvdpn srmwhrclts tgqpdfi*
```

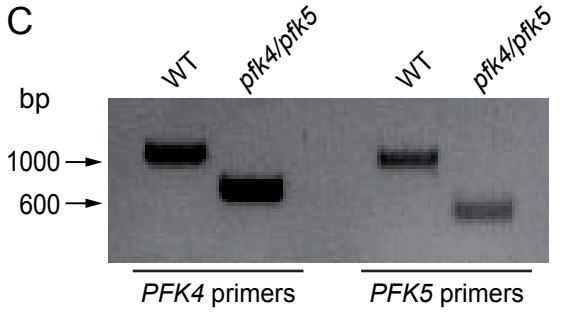

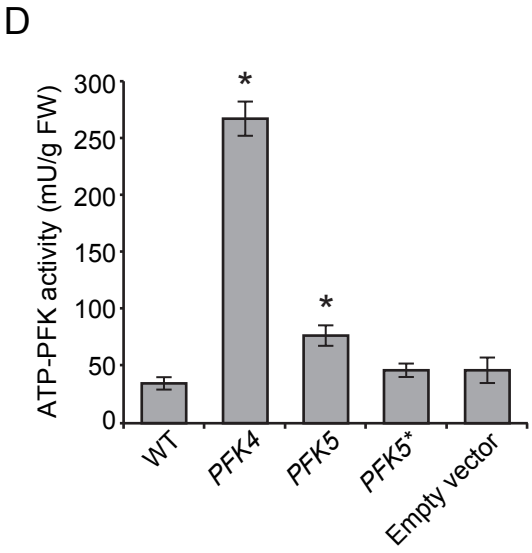

Supplemental Figure 5: Confirmation of the knock-out status of the *pfk4/pfk5* mutant**. (A)** Schematic illustration of the sites of T-DNA insertion in the *pfk4* (SALK_012602) and *pfk5* (SAIL_297_F05) alleles. **(B)** Deduced amino acid sequence of PFK5. The sequence that is not expressed in *pfk5* is highlighted in red. **(C)** PCR analyses of the *pfk4/pfk5* mutant. *PFK* LP and RP specific primers, and T-DNA specific primers used are listed in **Supplemental Table 1.** Annealing positions of *PFK* LP and RP specific primers, and T-DNA specific primers are shown in panel A. **(D)** ATP-PFK activities of tobacco leaves transiently expressing PFK4, PFK5 or PFK5*. Values represent the means ± SE obtained from three independent experiments, each consisting of three biological replicates corresponding to a pool of 4 agro-infiltrated tobacco leaves. Asterisks indicate significant differences from WT leaves according to Student´s t-tests (p<0.05). Note that PFK5 has weak activity, relative to PFK4, in accordance with findings by Mustroph et al. (2007). Note also that the truncated PFK5* form totally lacks ATP-PFK activity (**Supports Figure 8**).

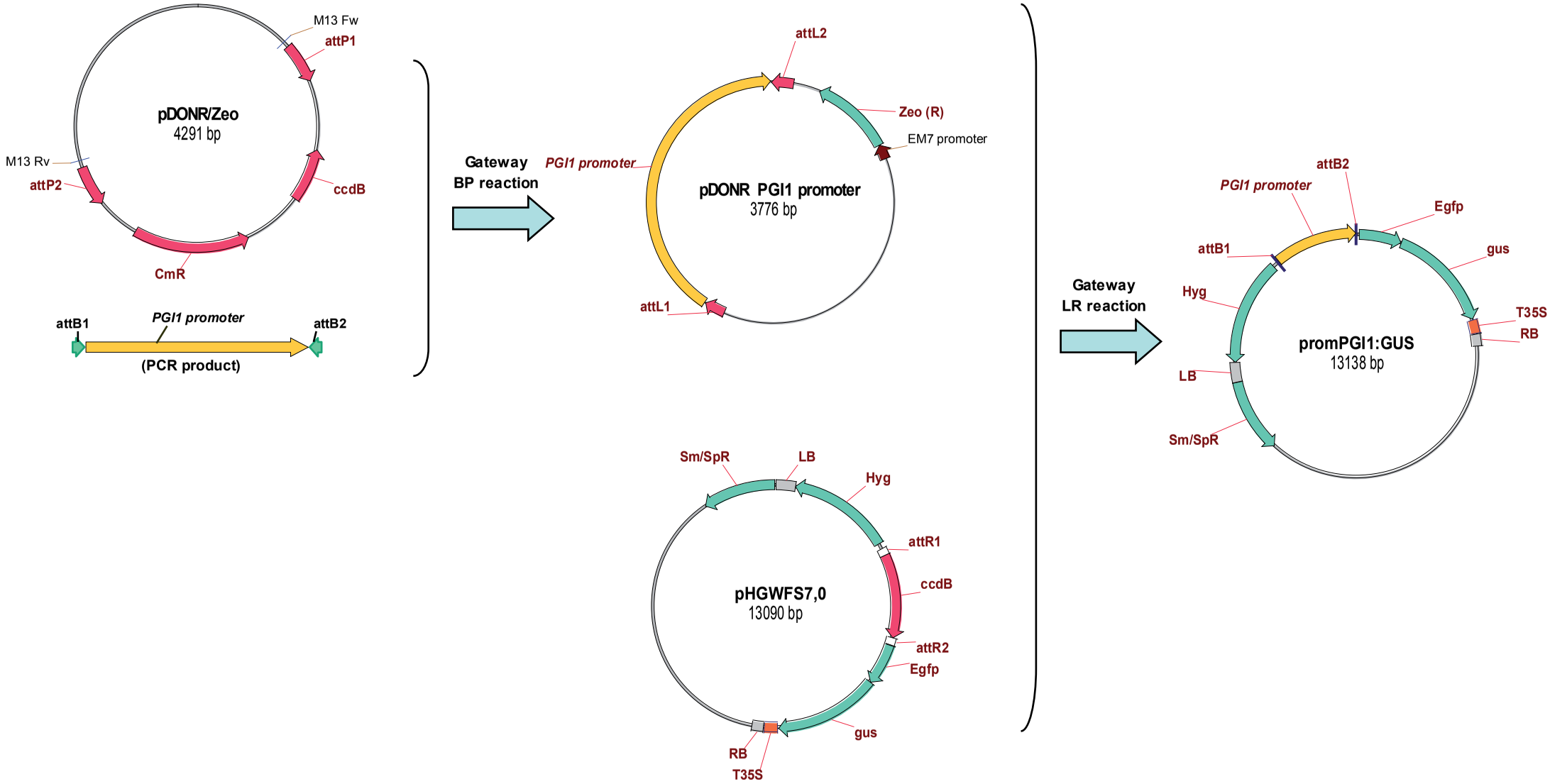

Supplemental Figure 6: Stages in construction of the promPGI1:GUS, 35S:PGI1 and promPGI1:PGI1 plasmids used to produce *promPGI1:GUS*-, *35S:PGI1*- and *promPGI1:PGI1*- expressing plants. Plasmid constructs were produced using Gateway technology and confirmed by sequencing. Complete PGI1-encoding cDNA was obtained from the RIKEN Arabidopsis cDNA collection (Seki et al., 1998; 2002). To construct *promPGI1-GUS* a 1.7-kb fragment of the *PGI1* upstream region was amplified by PCR and subcloned in front of the GUS reporter gene. Primers used for PCR amplification of *PGI1* cDNA, *GUS* and the *PGI1* promoter are listed in **Supplemental Table 2** (**Supports Figure 1**).

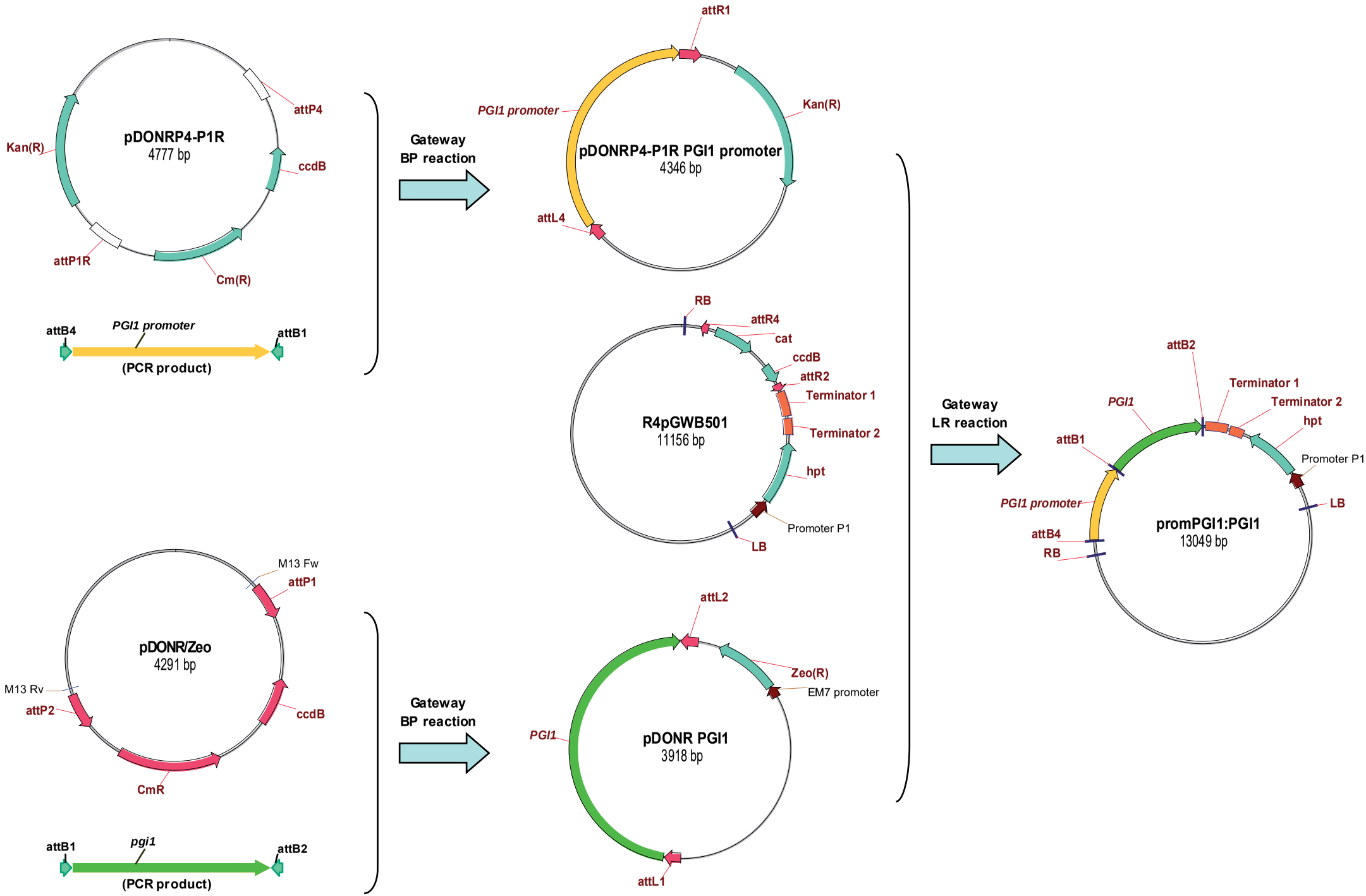
pDONRP4-P1R
4777 bp
attP4
Kan(R)
ccdB
attP1R
Cm(R)
attB4
PGI1 promoter
attB1
(PCR product)
Gateway
BP reaction
attR1
PGI1 promoter
Kan(R)
pDONRP4-P1R PGI1 promoter
4346 bp
attL4
RB
attR4
cat
ccdB
attR2
Terminator 1
Terminator 2
R4pGWB501
11156 bp
hpt
Promoter P1
LB
M13 Fw
attP1
pDONR/Zeo
4291 bp
M13 Rv
attP2
ccdB
CmR
attB1
pgi1
attB2
(PCR product)
Gateway
BP reaction
attL2
Zeo(R)
EM7 promoter
PGI1
pDONR PGI1
3918 bp
attL1
Gateway
LR reaction
attB2
Terminator 1
PGI1
Terminator 2
hpt
attB1
Promoter P1
PGI1 promoter
LB
promPGI1:PGI1
13049 bp
attB4
RB

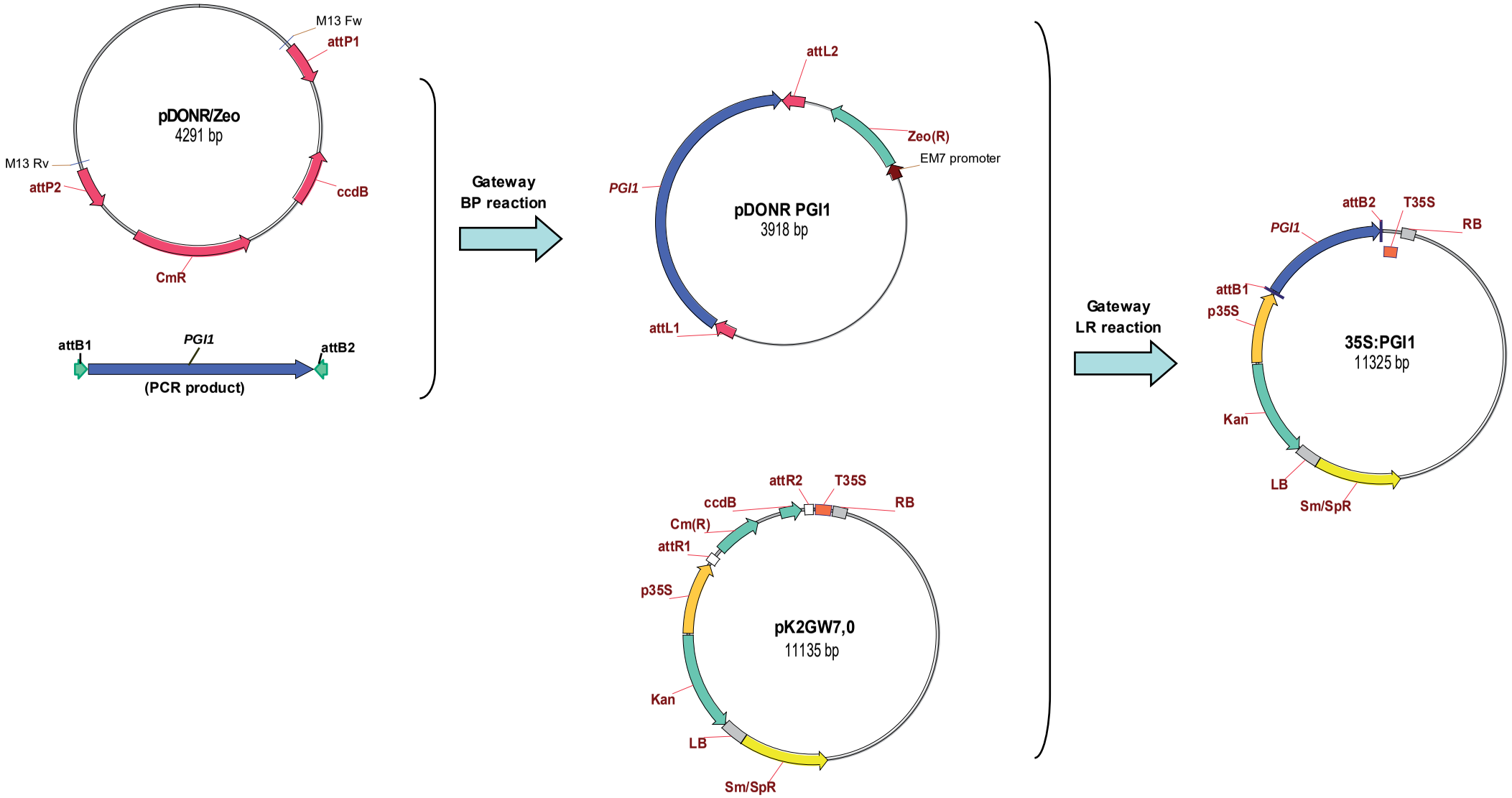
M13 Fw
attP1
pDONR/Zeo
4291 bp
M13 Rv
attP2
ccdB
CmR
attB1
PGI1
attB2
(PCR product)
Gateway
BP reaction
attL2
Zeo(R)
EM7 promoter
PGI1
pDONR PGI1
3918 bp
attL1
attR2
T35S
RB
ccdB
Cm(R)
attR1
p35S
pK2GW7,0
11135 bp
Kan
LB
Sm/SpR
Gateway
LR reaction
attB2
T35S
RB
PGI1
attB1
p35S
35S:PGI1
11325 bp
Kan
LB
Sm/SpR

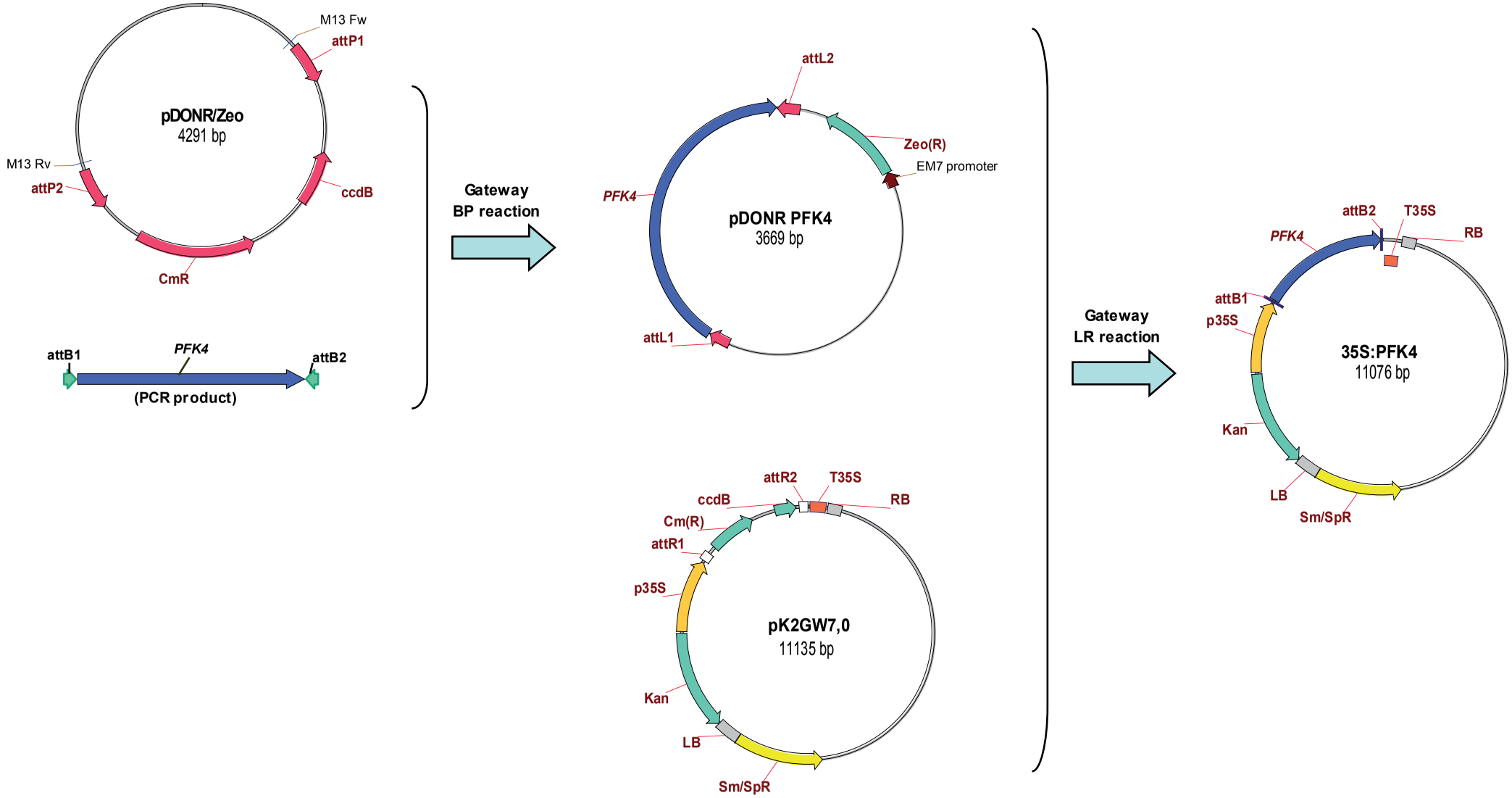

Supplemental Figure 7: Stages in construction of the 35S:PFK4, 35S:PFK5 and 35S:PFK5* plasmids used for transient expression in tobacco leaves. Plasmid constructs were produced using Gateway technology and confirmed by sequencing. Complete PFK4- and PFK5-encoding cDNAs were obtained from the RIKEN Arabidopsis cDNA collection (Seki et al., 1998; 2002). Primers used for PCR amplification of *PFK4, PFK5* and *PFK5** are listed in **Supplemental Table 2** (**Supports Figure 8**).

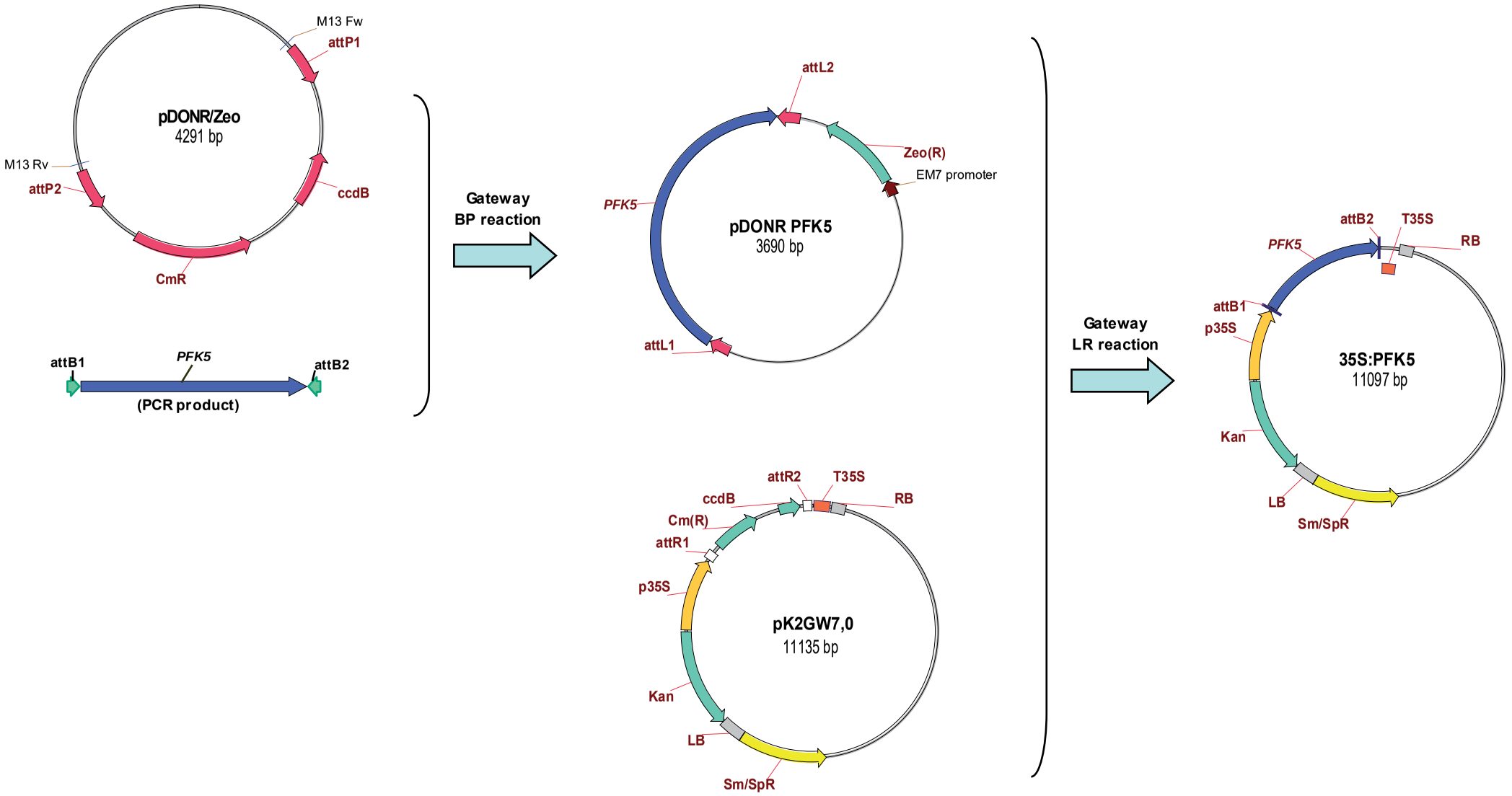
M13 Fw
attP1
pDONR/Zeo
4291 bp
M13 Rv
attP2
ccdB
CmR
attB1
PFK5
attB2
(PCR product)
Gateway
BP reaction
attL2
Zeo(R)
EM7 promoter
PFK5
pDONR PFK5
3690 bp
attL1
attR2
T35S
RB
ccdB
Cm(R)
attR1
p35S
pK2GW7,0
11135 bp
Kan
LB
Sm/SpR
Gateway
LR reaction
attB2
T35S
RB
PFK5
attB1
p35S
35S:PFK5
11097 bp
Kan
LB
Sm/SpR

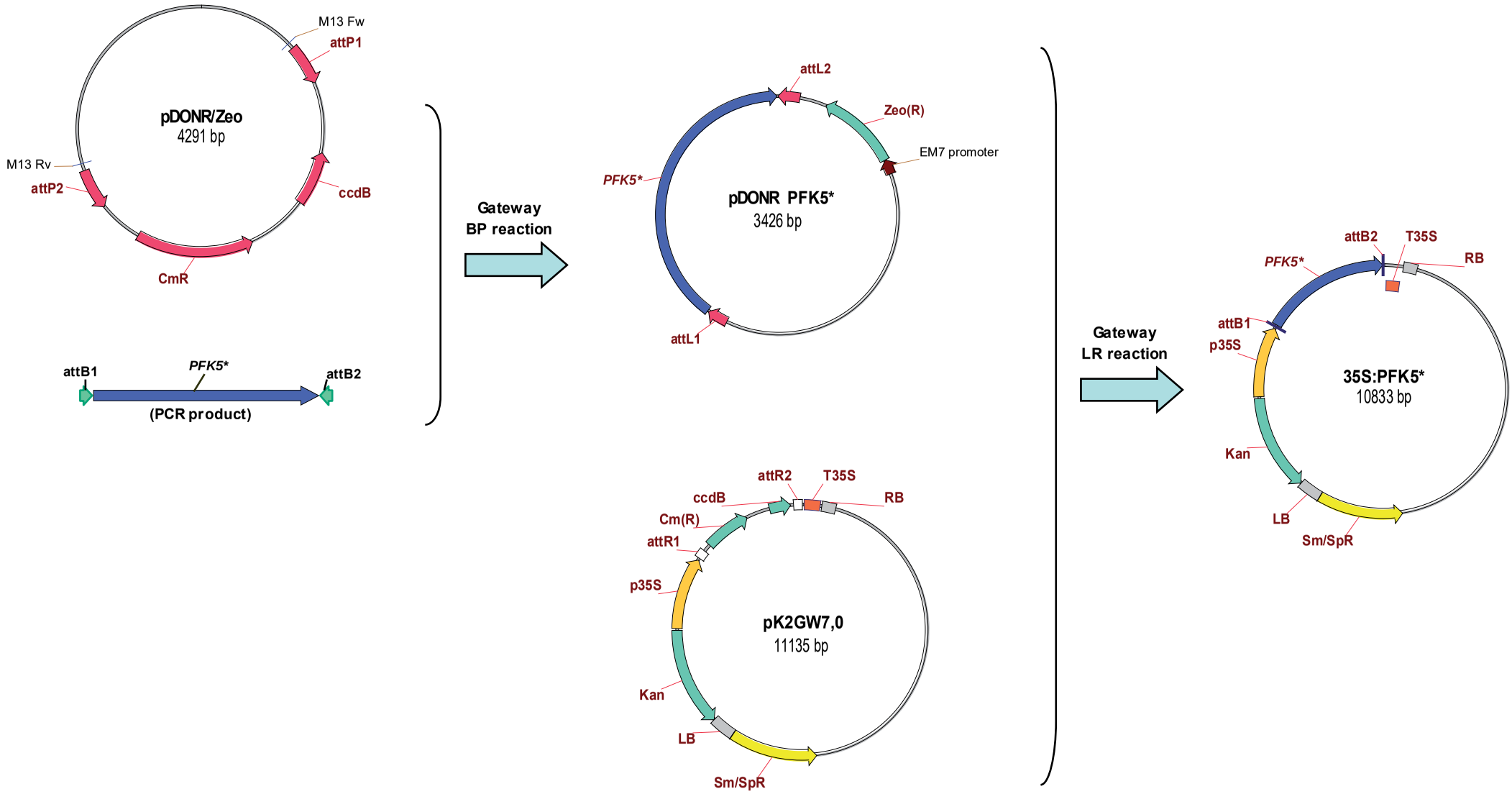
pDONR/Zeo
4291 bp
M13 Fw
attP1
M13 Rv
attP2
ccdB
CmR
attB1
PFK5*
attB2
(PCR product)
Gateway
BP reaction
pDONR PFK5*
3426 bp
attL2
Zeo(R)
EM7 promoter
PFK5*
attL1
pK2GW7,0
11135 bp
attR2
T35S
RB
ccdB
Cm(R)
attR1
p35S
Kan
LB
Sm/SpR
Gateway
LR reaction
35S:PFK5*
10833 bp
attB2
T35S
RB
PFK5*
attB1
p35S
Kan
LB
Sm/SpR

Supplemental Table 1. Primers used for PCR screening of the *pfk4 pfk5* mutant.

Mutant	**Primer**	**Sequence**
pfk4 (SALK_012602)	RP (*pfk4*)	5′ AGGCGAACTTTTGTCAGTTCC 3′
	LP (*pfk4*)	5′ ACCACTGTATCTGCCCATGAG 3′
	LBb1 (T-DNA)	5′ GCGTGGACCGCTTGCTGCAACT 3′
pfk5 (SAIL_297_F05)	RP (*pfk5*)	5′ TTTTAGATGAAATCGGGTTGG 3′
	LP (*pfk5*)	5′ TTTGGGCCTTCTGTATTAGGC 3′
	LB3 (T-DNA)	5′ TAGCATCTGAATTTCATAACCAATCTCGATACAC 3′

Supplemental Table 2. Primers used to produce the promPGI1:GUS, promPGI1:PGI1, 35S:PGI1, 35S:PFK4, 35S:PFK5 and 35S:PFK5* plasmids. Primer sequences for attB sites (see **Supplemental Figures 6 and 7**) are indicated in bold.

Primer	Sequence
promPGI1:GUS	
attB1 *PGI1* promoter	5′ **GGGGACAAGTTTGTACAAAAAAGCAGGCTTA**CTTTATATGATCCGATTCAATCTAAAC 3′
attB2 *PGI1* promoter	5′ **GGGGACCACTTTGTACAAGAAAGCTGGGTA**AAATTCTTGGCTCATTGAGAAGG 3′
promPGI1:PGI1	
attB4 *PGI1* promoter	5′ **GGGGACAACTTTGTATAGAAAAGTTGCT**CTTTATATGATCCGATTCAATCTAAAC 3′
attB1R *PGI1* promoter	5′ **GGGGACTGCTTTTTTGTACAAACTTGC**AAATTCTTGGCTCATTGAGAAGG 3′
attB1 *PGI1*	5′ **GGGGACAAGTTTGTACAAAAAAGCAGGCTTA**ATGGCCTCTCTCTCAGGC 3′
attB2 *PGI1*	5′ **GGGGACCACTTTGTACAAGAAAGCTGGGTA**TTATGCGTACAGGTCATCCAC 3′
35S:PGI1	
attB1 *PGI1*	5′ **GGGGACAAGTTTGTACAAAAAAGCAGGCTTA**ATGGCCTCTCTCTCAGGC 3′
attB2 *PGI1*	5′ **GGGGACCACTTTGTACAAGAAAGCTGGGTA**TTATGCGTACAGGTCATCCAC 3′
35S:PFK4	
attB1 *PFK4*	5′ **GGGGACAAGTTTGTACAAAAAAGCAGGCTTA**ATGGAAGCTTCGATTTCGTTTC 3′
attB2 *PFK4*	5′ **GGGGACCACTTTGTACAAGAAAGCTGGGTA**TTAGATAGAAGAGATCTTCATGTT 3′
35S:PFK5	
attB1 *PFK5*	5′ **GGGGACAAGTTTGTACAAAAAAGCAGGCTTA**ATGGATGCTCTTTCTCAGGCG 3′
attB2 *PFK5*	5′ **GGGGACCACTTTGTACAAGAAAGCTGGGTA**TTAGATGAAATCGGGTTGGCC 3′
35S:PFK5*	
attB1 *PFK5*	5′ **GGGGACAAGTTTGTACAAAAAAGCAGGCTTA**ATGGATGCTCTTTCTCAGGCG 3′
attB2 *PFK5**	5′ **GGGGACCACTTTGTACAAGAAAGCTGGGTA**TTAAGTACTTATTTCTTTGAAATACTTC 3′

Supplemental Table 3. Primers used in qRT-PCR analyses

Gene	Direction	Sequence
EF-1α RNA	Forward	5´ TTCTTGACAACACCGACAGC 3´
At1g07940	Reverse	5´ AAGCCCATGGTTGTTGAGAC 3´
PGI1	Forward	5´ GCTGCGTTTAAGGCTATGGA 3´
At4g24620	Reverse	5´ GGCTTAGGTGCGAGCTTAGA 3´
GA2ox1	Forward	5´ CCAAGTCTTCTCAAAAGCCCG 3´
At1g78440	Reverse	5´ GTACTCTTCCAATGCGTTTCTGAA 3´
GA2ox2	Forward	5´ GGTTCCGGTTCTCACTTCCC 3´
At1g30040	Reverse	5´ GGATCGGCTAGGTTGACGAC 3´
GA2ox3	Forward	5´ AGCCAGCCAGTTTTGATAGCA 3´
At2g34555	Reverse	5´ GCGGTTTGCATTTTGGATTAAC 3´
GA2ox4	Forward	5´ CTTTGCTAAACCGGCTCACG 3´
At1g47990	Reverse	5´ GGCTGGTTAACTGGTCGGAC 3´
GA2ox6	Forward	5´ GATCCTTTCAAGTTCAGCTCGG 3´
At1g02400	Reverse	5´ TCTAACCGTGCGTATGTAATCATTC 3´
GA2ox7	Forward	5´ ATGGACAATGGATCAGCGTAAA 3´
At1g50960	Reverse	5´ TGTTGACTGTAAGGGCTTCCAA 3´
GA2ox8	Forward	5´ CATGGAGCAATGGCATGTACA 3´
At4g21200	Reverse	5´ GGTTCGTCATCACACGGTGTT 3´
GA3ox1	Forward	5´ CCATTCACCTCCCACACTCT 3´
At1g15550	Reverse	5´ AGCGGAGAAGAGGAGATCGT 3´
GA3ox2	Forward	5´ CTGCCGCTCATCGACCTC 3´
At1g80340	Reverse	5´ AGCATGGCCCACAAGAGTG 3´
GA3ox3	Forward	5´ CGCTACACTCTTATGGCCCG 3´
At4g21690	Reverse	5´ TCCATCACATTGCAGAACTCG 3´
GA3ox4	Forward	5´ GATCACACCAAGTACTGCGGTATAA 3´
At1g80330	Reverse	5´ TTCCATTTCGTCCACGTATTCTT 3´
GA20ox1	Forward	5´ CTTCCATCAACGTTCTCGAGC 3´

At4g25420	Reverse	5´ GGTTTTGAAGGTCGATGAGAGG 3´

GA20ox2	Forward	5´ AGAAACCTTCCATTGACATTCCA 3´
At5g51810	Reverse	5´ AGAGATCGATGAACGGGACG 3´
GA20ox3	Forward	5´ ACTCGTCTCAAAGGCTGCAAC 3´
At5g07200	Reverse	5´ GAGGCTCTCATCGACACCATG 3´
GA20ox4	Forward	5´ CTATCCAAAATGCAAGCAACCA 3´
At1g60980	Reverse	5´ CAGTGAGGCCCCGTACCTAGT 3´
GA20ox5	Forward	5´ GCCACCCCATGTTGTTGAAG 3´
At1g44090	Reverse	5´ CGATGGTTGCCTAGCCTTGA 3´

Supplemental Table 4. ANOVA Tables

Figure 3

df = degrees of freedom; Mean Sq = Mean Squares; Sum Sq = Sum of Squares

GA1

	df	Sum Sq	Mean Sq	F-value	P-value
Treatment	1	5.33571	5.33571	50.51	0.0004***
Residual	6	0.6338	0.10563		
Total	7	5.9695			

GA4

	df	Sum Sq	Mean Sq	F-value	P-value
Treatment	1	0.23823	0.23823	9.09	0.0236*
Residual	6	0.15729	0.02621		
Total	7	0.39552			

GA5

	df	Sum Sq	Mean Sq	F-value	P-value
Treatment	1	0	0	5.41e-05	0.9944
Residual	6	0.03864	0.00644		
Total	7	0.03864			

GA6

	df	Sum Sq	Mean Sq	F-value	P-value
Treatment	1	0.00122	0.00122	0.08	0.7932
Residual	6	0.09726	0.01621		
Total	7	0.09847			

GA7

	df	Sum Sq	Mean Sq	F-value	P-value
Treatment	1	0.00002	0.00002	0.01	0.907
Residual	6	0.00833	0.00139		
Total	7	0.00835			

GA8

	df	Sum Sq	Mean Sq	F-value	P-value
Treatment	1	8.4912	8.49122	18.49	0.0051**
Residual	6	2.7557	0.45919		
Total	7	11.2464			

GA9

	df	Sum Sq	Mean Sq	F-value	P-value
Treatment	1	0.09103	0.09103	0.09	0.7721
Residual	6	5.94785	0.99131		
Total	7	6.03888			

GA15

	df	Sum Sq	Mean Sq	F-value	P-value
Treatment	1	0.06504	0.06504	14.01	0.0096**
Residual	6	0.02785	0.00464		
Total	7	0.09289			

GA19

	df	Sum Sq	Mean Sq	F-value	P-value
Treatment	1	0.01987	0.01987	0.05	0.8354
Residual	6	2.5335	0.42225		
Total	7	2.55338			

GA20

	df	Sum Sq	Mean Sq	F-value	P-value
Treatment	1	1.82745	1.82745	6.54	0.0431*
Residual	6	1.67781	0.27964		
Total	7	3.50527			

GA24

	df	Sum Sq	Mean Sq	F-value	P-value
Treatment	1	1.30947	1.30947	1.1	0.3344
Residual	6	7.13448	1.18908		
Total	7	8.44395			

GA29

	df	Sum Sq	Mean Sq	F-value	P-value
Treatment	1	50.9593	50.9593	68.12	0.0002***
Residual	6	4.4886	0.7481		
Total	7	55.4479			

GA34

	df	Sum Sq	Mean Sq	F-value	P-value
Treatment	1	0.00161	0.00161	0.69	0.4371
Residual	6	0.01393	0.00232		
Total	7	0.01553			

GA44

	df	Sum Sq	Mean Sq	F-value	P-value
Treatment	1	0.20416	0.20416	0.56	0.481
Residual	6	2.17092	0.36182		
Total	7	2.37508			

GA51

	df	Sum Sq	Mean Sq	F-value	P-value
Treatment	1	0.90201	0.90201	3.55	0.1086
Residual	6	1.52578	0.2543		
Total	7	2.42779			

SUPPLEMENTAL REFERENCES

Mustroph, A., Sonnewald, U., and Biemelt, S. (2007). Characterization of the ATP-dependent phosphofructokinase gene family from *Arabidopsis thaliana*. FEBS Lett. 581: 2401-2410.

Seki, M., Carninci, P., Nishiyama, Y., Hayashizaki, Y. and Shinozaki, K. (1998) High-efficiency cloning of Arabidopsis full-length cDNA by biotinylated CAP trapper. Plant J. 15: 707-720.

Seki, M., Narusaka, M., Kamiya, A., Ishida, J., Satou, M., Sakurai, T., Nakajima, M., Enju, A., Akiyama, K., Oono, Y., Muramatsu, M., Hayashizaki, Y., Kawai, J., Carninci, P., Itoh, M., Ishii, Y., Arakawa, T., Shibata, K., Shinagawa, A., and Shinozaki K (2002) Functional annotation of a full-length Arabidopsis cDNA collection. Science 296: 141-145.